

# Options on Interbank Rates and Implied Disaster Risk<sup>\*</sup>

Hitesh Doshi<sup>†</sup>

Hyung Joo Kim<sup>‡</sup>

Sang Byung Seo<sup>§</sup>

July 8, 2025

## Abstract

The identification of disaster risk has remained a significant challenge due to the rarity of macroeconomic disasters. We show that the interbank market can help characterize the time variation in disaster risk. We propose a risk-based model in which macroeconomic disasters are likely to coincide with interbank market failure. Using interbank rates and their options, we estimate our model via MLE and filter the short-run and long-run components of disaster risk. Our estimation results are independent of the stock market and serve as an external validity test of rare disaster models, which are typically calibrated to match stock moments.

---

<sup>\*</sup>We thank George Pennacchi (the editor) and the anonymous referee for their valuable comments and suggestions. We are also grateful to Caio Almeida, Hui Chen, Mathieu Fournier, Kris Jacobs, Mete Kilic, Praveen Kumar, Ivan Shaliastovich, Anders Trolle, Jessica Wachter, Nancy Xu, and seminar participants at the North American Summer Meeting of the Econometric Society, European Finance Association Annual Meeting, Northern Finance Association Conference, Financial Management Association Annual Meeting, and University of Houston for helpful comments. We gratefully acknowledge the financial support from the Canadian Derivatives Institute. The analysis and conclusions set forth are those of the authors and do not indicate concurrence by the Federal Reserve Board or other members of its staff. An earlier version of this manuscript was circulated under the title “What Interbank Rates Tell Us About Time-Varying Disaster Risk.”

<sup>†</sup>Bauer College of Business, University of Houston; hdoshi@bauer.uh.edu

<sup>‡</sup>Federal Reserve Board of Governors; hyungjoo.kim@frb.gov

<sup>§</sup>Wisconsin School of Business, University of Wisconsin-Madison; sang.seo@wisc.edu

# 1 Introduction

Severe macroeconomic contractions are often accompanied by widespread financial sector distress. Historical events such as the Great Depression illustrate how disruptions in the banking system can trigger or amplify economic collapse (Bernanke, 1983). More recent empirical work supports this view, showing that defaults in the financial sector, unlike those in non-financial sectors, are closely tied to macroeconomic downturns (Allen, Bali, and Tang, 2012; Giesecke, Longstaff, Schaefer, and Strebulaev, 2014). The association between macroeconomic and financial crises is particularly strong for extreme episodes: as noted by Reinhart and Rogoff (2013), virtually all consumption disasters documented by Barro and Ursúa (2008) were coupled with systemic banking crises.

In this paper, we exploit this empirical regularity to propose a new method for estimating the risk of rare economic disasters. Macro-finance models featuring disaster risk have become a popular framework for capturing macroeconomic tail risk and explaining prominent asset pricing puzzles.<sup>1</sup> Yet, the rare disaster literature faces a major empirical challenge. Disasters are often referred to as “dark matter” because of their rarity and the obscurity of their source. This criticism points to the fact that it is difficult to reliably estimate the parameters associated with disasters, based on the historical consumption time series.<sup>2</sup> Estimating time-varying disaster risk is even more difficult; Cochrane (2017) describes time-varying disaster probabilities as “dark energy,” unless they can be independently anchored to external data.

We address these limitations by using interbank rates and their options. Our key assump-

---

<sup>1</sup>In order to describe an extreme and rare economic downturn, the literature defines macroeconomic disasters as a severe drop in real consumption per capita (e.g., Barro, 2006; Barro and Ursúa, 2008; Gabaix, 2012; Wachter, 2013) or as a significant reduction in total factor productivity (e.g., Gourio, 2012).

<sup>2</sup>In line with this, Chen, Dou, and Kogan (2024) raise concerns about overfitting in-sample data: if a model overfits, its implications become highly sensitive to small perturbations in disaster parameters.

tion is that macroeconomic disasters are likely to coincide with interbank market failure – a view supported by historical data. This assumption provides a direct link between disaster risk and observed prices in the interbank market. We show that interbank rates and their options allow us to characterize the time series evolution of disaster risk, with the aid of a model.

For our analysis, we adopt a risk-based model where the nominal pricing kernel is affine and is comprised of Brownian and Poisson shocks to five state variables of the economy: real consumption growth, mean consumption growth, expected inflation, short-run disaster risk, and long-run disaster risk. This framework allows us to derive the expressions for three distinct interest rates: (i) interbank rate (LIBOR), (ii) risk-free rate (proxied by the OIS rate), and (iii) government bill rate (Treasury rate).

Within our model, risk-free lending always pays back the promised amount at the end of its maturity, whereas interbank lending is potentially subject to partial defaults in the event of a disaster. Consequently, their interest rate difference, the so-called LIBOR-OIS spread, is highly informative about disaster risk, directly reflecting the two disaster-related state variables. We also show that the spread between the interbank rate and the Treasury rate, commonly referred to as the TED spread, can serve as a useful indicator of disaster risk. However, its signal may be noisier than the LIBOR-OIS spread due to the complexity arising from the Treasury convenience yield. Following recent studies on safe/liquid assets, we assume that government bills may carry a convenience yield in our model, causing the Treasury rate to be, on average, lower than the risk-free rate.

In addition to the two interest rate spreads, we take advantage of interest rate caps and swaptions. We approach these financial instruments from a new angle. Prior studies simply

consider them as option contracts on future benchmark interest rates, often overlooking the aspect that the underlying rates are not default-free. In contrast, we view them as options on future interbank rates: a cap consists of a series of caplets, each of which is a call option on the LIBOR; a swaption provides its holder the right to enter into an interest rate swap that exchanges fixed coupons with floating coupons based on the LIBOR. Naturally, these instruments reflect the possibility of interbank market failure and hence that of economic disasters. We believe that this is an important distinction because, as witnessed during the 2008 financial crisis, interbank rates can significantly deviate from default-free interest rates.

We estimate the model parameters via maximum likelihood estimation using the data from February 2002 to December 2019. As a result, we obtain parameter estimates whose signs and magnitudes are economically sensible. The model-implied time series for interest rates, caps, and swaptions mimic their data counterparts reasonably well. Our results provide additional guidelines that can help discipline the calibration of rare disaster models.

An important advantage of our estimation is that it is possible to extract the short-run and long-run components of latent disaster risk through a filtering approach. Specifically, we adopt the unscented Kalman filter because caps and swaption prices are nonlinear functions of the latent and observable state variables.<sup>3</sup> From a sensitivity analysis, we discover that the short-run component of disaster risk is mainly identified by the LIBOR-OIS spread with a short maturity. In contrast, the long-run component of disaster risk is primarily filtered through caps and swaptions whose payoffs are contingent on future interbank rates over a long horizon. Importantly, the forward-looking information from interest rate options plays a

---

<sup>3</sup>The unscented Kalman filter has been widely used in filtering latent variables from nonlinear financial asset prices. See, for instance, Filipović and Trolle (2013), Christoffersen, Dorion, Jacobs, and Karoui (2014), Park (2016), Doshi, Elkamhi, and Ornathanalai (2018), and Bakshi, Crosby, Gao, and Hansen (2023).

crucial role in estimating the whole dynamics of disaster risk.

Additionally, based on the filtered time series of the short-run and long-run components of disaster risk, we verify the testable implications that disaster risk is associated with conditional moments and returns in the equity market. We find that higher disaster risk is generally linked to lower stock market valuations, in terms of the price-dividend and price-earnings ratios. Intuitively, the short-run component of disaster risk significantly explains implied variance, expected realized variance, and the variance risk premium over the next month, as well as short-maturity out-of-the-money put option prices. The long-run component, however, becomes more relevant for longer-horizon moments. Shocks to disaster risk are also negatively associated with prominent equity return factors, such as market, size, and liquidity, and have stronger negative effects on returns for cyclical industries.

Overall, our results demonstrate that the interbank market can potentially be useful for overcoming the criticisms of rare disaster models, which are typically calibrated to match stock data. Our estimation is independent of equity market moments and, thus, serves as an external/out-of-sample validity test of the models. The estimation results suggest that disaster risk is significant in magnitude and in variation, strongly supporting macro-finance models with the rare disaster mechanism.

Our paper relates to several strands of the literature.<sup>4</sup> We contribute to the rare disaster literature by estimating the time-varying risk of economic disasters. Granted, we are not the first to attempt to quantify the time series variation in disaster risk. For example, Berkman, Jacobsen, and Lee (2011) proxy the perceived disaster probability by a crisis severity index,

---

<sup>4</sup>In the Internet Appendix, we provide detailed comparisons with related papers in table format, highlighting our modeling innovations and empirical contributions.

constructed based on the number of international political crises. Manela and Moreira (2017) create a text-based disaster concern measure, called news implied volatility (NVIX), using the words in front-page articles of the Wall Street Journal.<sup>5</sup> Rather than proposing another index that potentially correlates with disaster risk, our goal is to directly estimate the risk of consumption disasters under the assumption that consumption disasters are likely to coincide with interbank market failure. A key advantage of our framework is that it is possible to exploit the information contained in interbank rates and their options, which allows us to separately extract the short-run and long-run components of disaster risk.

Our estimation relies on the pricing data on interest rate caps and swaptions. Prior studies, including Longstaff, Santa-Clara, and Schwartz (2001), Han (2007), and Trolle and Schwartz (2009), mainly concentrate on the relative pricing of caps and swaptions. However, the literature has paid little attention to what these financial instruments imply about the aggregate economy or other financial markets. We explore the economic content of caps and swaptions by focusing on the fact that their payoffs are contingent on future interbank rates. We confirm that interbank rate options indeed contain valuable information about the risk of economic disasters.

The findings of this paper also potentially relate to the growing literature on the role of financial intermediaries in asset pricing. He and Krishnamurthy (2013) and Brunnermeier and Sannikov (2014) argue that intermediaries, rather than households, act as marginal investors and, therefore, their financial constraints serve as key drivers of market risk premia. Adrian,

---

<sup>5</sup>Related, Bollerslev and Todorov (2011a), Bollerslev and Todorov (2011b), Bollerslev and Todorov (2014), and Andersen, Fusari, and Todorov (2015) estimate and study the risk of rare events in the equity market using an essentially model-free approach based on high-frequency index time series and/or short maturity out-of-the-money index options. Bakshi, Gao, and Xue (2023) define a disaster as an event in which the equity market declines over a certain threshold and estimate its probability using S&P 500 options.

Etula, and Muir (2014) and He, Kelly, and Manela (2017) empirically support this theory by showing that intermediary-induced factors outperform traditional risk factors in explaining asset returns in various markets. Although our analysis mainly concerns economic disasters, the pricing kernel we adopt has properties that are isomorphic to those of an intermediary-based pricing kernel: when the interbank market is hit by a shock (which is modeled as a shock to disaster risk in our framework), the pricing kernel responds and amplifies risk premia. Our results hint that the disaster-based explanation and the intermediary-based explanation of asset markets might share common microfoundations.

The rest of this paper proceeds as follows. Section 2 describes the model. Section 3 describes the data as well as explains how we estimate the model and extract time-varying disaster risk. Section 4 reports the estimation results and discusses their implications. Section 5 concludes.

## 2 Model

### 2.1 Risk of disasters and interbank rates

How can we characterize the time-varying risk of economic disasters? In this section, we illustrate how interbank rates can help. Let  $C_t$  denote aggregate real consumption, which follows an affine jump diffusion process:

$$\frac{dC_t}{C_{t-}} = \mu_t dt + \sigma_C dB_{C,t} + (e^{Z_{C,t}} - 1) dN_t,$$

where  $B_{C,t}$  is a standard Brownian motion. The occurrence of consumption disasters is specified by a Poisson process  $N_t$  with a negative jump size random variable  $Z_{C,t}$ : when a consumption disaster occurs ( $dN_t = 1$ ), consumption falls from  $C_{t-}$  to  $C_{t-}e^{Z_{C,t}}$ . Given this setup, our main objective is to properly estimate the time series of the intensity process for  $N_t$ . We assume that  $N_t$  has stochastic intensity  $\lambda_t$  whose dynamics are described by

$$\begin{aligned} d\lambda_t &= \kappa_\lambda(\xi_t - \lambda_t)dt + \sigma_\lambda\sqrt{\lambda_t}dB_{\lambda,t}, \\ d\xi_t &= \kappa_\xi(\bar{\xi} - \xi_t)dt + \sigma_\xi\sqrt{\xi_t}dB_{\xi,t}, \end{aligned}$$

where  $\xi_t$  is the time-varying mean of  $\lambda_t$ . Simply put,  $\lambda_t$  and  $\xi_t$  represent the short-run and long-run components of disaster risk. In the absence of a disaster ( $dN_t = 0$ ), the consumption dynamics simply reduce to a Geometric Brownian motion with time-varying mean  $\mu_t$  and constant volatility  $\sigma_C$ , where

$$d\mu_t = \kappa_\mu(\bar{\mu} - \mu_t)dt + \sigma_\mu dB_{\mu,t}.$$

That is, mean consumption growth in normal-times  $\mu_t$  reverts to its long-run mean  $\bar{\mu}$  at the rate of  $\kappa_\mu$ , while experiencing random Brownian shocks  $dB_{\mu,t}$  with volatility coefficient  $\sigma_\mu$ .

We study the time series evolution of  $\lambda_t$  and  $\xi_t$  by linking consumption disasters to the banking sector. As evident in the example of the Great Depression, the collapse of the banking sector is closely related to severe economic downturns. In fact, Reinhart and Rogoff (2013) point out that virtually all consumption disasters documented by Barro and Ursúa (2008) were accompanied by severe systemic banking crises. Motivated by this insight, we assume



that consumption disasters are likely to coincide with extreme rare events where the interbank market fails and market participants suffer significant losses.

More formally, let  $L_t$  denote the time- $t$  face value of interbank lending. We assume that in the event of a consumption disaster, the interbank market fails with probability  $\bar{p}$ , which results in a loss to the lenders:

$$L_t = \begin{cases} L_{t-} e^{Z_{L,t}} & \text{with probability } \bar{p} \text{ if a disaster occurs at time } t, \\ L_{t-} & \text{otherwise.} \end{cases}$$

That is, the face value, or the expected principal payment from interbank lending, reduces from  $L_{t-}$  to  $L_{t-} e^{Z_{L,t}}$  if the interbank market fails.<sup>6</sup> By defining  $I_t$  as a Bernoulli random variable with success probability  $\bar{p}$ , we can express the dynamics of  $L_t$  as

$$\frac{dL_t}{L_{t-}} = (e^{Z_{L,t} I_t} - 1) dN_t. \quad (1)$$

Here, we do not model the behaviors of banks nor the structure of the interbank market, which can potentially generate consumption disasters and interbank market failure in an endogenous fashion. Moreover, we are agnostic about any causal link: whether interbank market failure leads to consumption disasters or vice versa, and through which mechanism they are related. Since our focus is on empirically characterizing time-varying disaster risk, it suffices that these two types of extreme events are likely to coincide with each other.

Under this simple setup, it is intuitive that the spread between the interbank rate and the risk-free rate contains important information about disaster risk. The pricing relation implies

---

<sup>6</sup>The reduced-form way in which we model risky interbank lending is reminiscent of fractional-loss-at-default models in the spirit of Duffie and Singleton (1999) and Duffie (2005).

that the  $\tau$ -maturity zero-coupon interbank rate can be derived as

$$y_{i,t}^{(\tau)} = -\frac{1}{\tau} \log \mathbb{E}_t \left[ \frac{M_{t+\tau}}{M_t} \cdot \frac{L_{t+\tau}}{L_t} \right], \quad (2)$$

where  $\frac{M_{t+\tau}}{M_t}$  represents the nominal pricing kernel whose existence is guaranteed under no arbitrage. While interbank lending contracts are potentially subject to partial defaults, risk-free lending always pays back the promised amount at the end of their maturity. The  $\tau$ -maturity zero-coupon risk-free rate is calculated as

$$y_{f,t}^{(\tau)} = -\frac{1}{\tau} \log \mathbb{E}_t \left[ \frac{M_{t+\tau}}{M_t} \cdot 1 \right]. \quad (3)$$

Comparing equations (2) and (3) suggests that changes in disaster risk have a direct effect on the interest rate spread  $y_{i,t}^{(\tau)} - y_{f,t}^{(\tau)}$ . When disaster risk rises, the expectation of the future payoff  $\frac{L_{t+\tau}}{L_t}$  decreases, which pushes the interbank rate upward. However, this effect is missing for the risk-free rate as the future payoff from a default-free bond is, by definition, always 1. As a result, the spread between the two interest rates widens when disaster risk increases.

These equations also suggest that fluctuations in disaster risk or in other potential risk factors can have indirect effects on the interbank rate and the risk-free rate through the pricing kernel. However, if risk factors only impact the pricing kernel but not the future payoff  $\frac{L_{t+\tau}}{L_t}$ , they will move the interbank rate with the same degree as the risk-free rate, leaving the spread between the two unchanged. As clear in equation (1), the distribution  $\frac{L_{t+\tau}}{L_t}$  only depends on instantaneous disaster risk  $\lambda_t$  and its time-varying mean  $\xi_t$ , and this suggests that risk factors that are orthogonal to  $\lambda_t$  and  $\xi_t$  will have no impact on the interest rate spread  $y_{i,t}^{(\tau)} - y_{f,t}^{(\tau)}$ . In

Section 2.3, we show that this spread indeed depends only on  $\lambda_t$  and  $\xi_t$  in our fairly flexible setup, confirming this intuition.

## 2.2 Nominal pricing kernel

Equations (2) and (3) make it clear that we need a nominal pricing kernel  $\frac{M_{t+\tau}}{M_t}$  to derive the expressions for zero-coupon yields. Rather than deriving it from investors' preferences as in typical equilibrium models, we take a reduced-form approach and directly specify the nominal pricing kernel. To this end, we first establish the state variables in the economy. In addition to real consumption ( $C_t$ ), mean consumption growth ( $\mu_t$ ), and the short-run/long-run components of disaster risk ( $\lambda_t, \xi_t$ ), we take one more variable that is typically used to capture the state of the nominal economy: expected inflation. This is particularly relevant, as we examine the term structure of nominal interest rates. In our model, the expected inflation process  $q_t$  solves the following stochastic differential equation:

$$dq_t = \kappa_q(\bar{q} - q_t)dt + \sigma_q dB_{q,t} + Z_{q,t}dN_t,$$

where  $B_{q,t}$  is another standard Brownian motion. Motivated by Tsai (2015), we assume that  $q_t$  is also subject to the same Poisson process  $N_t$  and that the jump size random variable  $Z_{q,t}$  is, on average, positive.<sup>7</sup>

We specify our pricing kernel in a general form so that it can be directly estimated using data. We assume that Brownian shocks  $(dB_{C,t}, dB_{\mu,t}, dB_{\lambda,t}, dB_{\xi,t}, dB_{q,t})$  are independent

---

<sup>7</sup>Since jumps in consumption and expected inflation always occur together through  $N_t$ , our model cannot generate inflation spikes that are not accompanied by disasters. In fact, Tsai (2015) adopts an additional Poisson process to capture such independent inflation spikes. Given our focus on studying disaster risk, we choose a more parsimonious setup and abstract away from this additional feature.

of one another and of a Poisson shock ( $dN_t$ ). These six independent shocks to the five state variables ( $C_t, \mu_t, \lambda_t, \xi_t, q_t$ ) are priced and hence constitute the nominal pricing kernel:

$$\begin{aligned} \frac{dM_t}{M_t^-} = & -r_t dt - \theta_C dB_{C,t} - \theta_\mu dB_{\mu,t} - \theta_\lambda \sqrt{\lambda_t} dB_{\lambda,t} - \theta_\xi \sqrt{\xi_t} dB_{\xi,t} - \theta_q dB_{q,t} \\ & + (e^{\theta_N Z_{C,t}} - 1) dN_t - \lambda_t \mathbb{E} [e^{\theta_N Z_{C,t}} - 1] dt, \quad (4) \end{aligned}$$

where  $(\theta_C, \theta_\mu, \theta_\lambda, \theta_\xi, \theta_q, \theta_N)$  indicate the market prices of risk and  $r_t$  represents the instantaneous nominal risk-free rate.<sup>8</sup> To preserve the affine structure of our setup, we represent the short rate  $r_t$  as a linear function of the state variables, similar to Ang and Piazzesi (2003) and Joslin, Le, and Singleton (2013):

$$r_t = \delta_0 + \delta_\lambda \lambda_t + \delta_\xi \xi_t + \delta_\mu \mu_t + \delta_q q_t. \quad (5)$$

The pricing kernel fully characterizes the risk-neutral measure, as the Radon-Nikodym derivative process of the risk-neutral measure with respect to the physical measure equals  $M_t \int_0^t r_s ds$ . In Appendix A.1, we derive the risk-neutral dynamics of the underlying processes using Girsanov's theorem.

Based on the pricing kernel specified in equation (4), we finally calculate the expressions for  $y_{i,t}^{(\tau)}$  and  $y_{f,t}^{(\tau)}$  in equations (2) and (3). We show that both interbank rates and Treasury

---

<sup>8</sup>The jump term  $(e^{\theta_N Z_{C,t}} - 1) dN_t$  in the pricing kernel captures the idea that there is a very high marginal utility state, which we call a disaster. A common econometric challenge in the disaster literature is that it is very difficult to separately identify the market price of risk  $\theta_N$  and the size distribution of disasters  $Z_{C,t}$ , as we do not observe any disaster realizations in the post-war sample. In our estimation, we set  $Z_{C,t}$  to the empirical distribution of real consumption disasters compiled by Barro and Ursúa (2008). This not only helps identify  $\theta_N$  but also allows us to interpret the estimated intensity of the Poisson process  $N_t$  as the probability/frequency of consumption disasters.

rates are linear in state variables  $\lambda_t$ ,  $\xi_t$ ,  $\mu_t$ , and  $q_t$ :

$$y_{i,t}^{(\tau)} = -\frac{1}{\tau} \left[ a_i(\tau) + b_{i,\lambda}(\tau)\lambda_t + b_{i,\xi}(\tau)\xi_t + b_\mu(\tau)\mu_t + b_q(\tau)q_t \right], \quad (6)$$

$$y_{f,t}^{(\tau)} = -\frac{1}{\tau} \left[ a_f(\tau) + b_{f,\lambda}(\tau)\lambda_t + b_{f,\xi}(\tau)\xi_t + b_\mu(\tau)\mu_t + b_q(\tau)q_t \right], \quad (7)$$

where deterministic functions  $a_i$ ,  $a_f$ ,  $b_{i,\lambda}$ ,  $b_{f,\lambda}$ ,  $b_{i,\xi}$ ,  $b_{f,\xi}$ ,  $b_\mu$  and  $b_q$  solve the ordinary differential equations in Appendix A.2.

## 2.3 Interest rate spreads

One important aspect when comparing equations (6) and (7) is that the loadings on mean consumption growth  $\mu_t$  and expected inflation  $q_t$  are identical for both types of interest rates. Therefore, for a given maturity  $\tau$ , the difference between  $y_{i,t}^{(\tau)}$  and  $y_{f,t}^{(\tau)}$  becomes a function of disaster risk  $(\lambda_t, \xi_t)$  alone, consistent with the intuition developed in Section 2.1. In our analysis, the data counterparts of the interbank rate and the risk-free rate are the London interbank offered rate (LIBOR) and the overnight index swap (OIS) rate, respectively, after being adjusted for compounding frequencies.<sup>9</sup> Thus, we can see that the spread between the (continuously compounded) LIBOR and OIS rate, the so-called LIBOR-OIS spread, can be

---

<sup>9</sup>Rigorously speaking, the OIS rates are not risk free, as they are derived from overnight index swaps based on the effective federal funds rate. Given that this is the rate at which banks borrow/lend their reserves on an uncollateralized basis, the OIS rates can essentially be seen as a “continually-refreshed” overnight interbank rate (Hull and White, 2015). Despite this, the OIS rates are widely used as a primary proxy for risk-free interest rates, especially in derivative markets. While the federal funds seller faces overnight credit risk, this is often considered very small, though not negligible, given the short maturity (and the fact that the buyer is another bank). Another contributing factor is that the effective federal funds rate is directly influenced by the Federal Reserve and has not deviated significantly from the target range since the 2000s.

expressed by

$$\text{LOIS}_t^{(\tau)} = -\frac{1}{\tau} \left[ (a_i(\tau) - a_f(\tau)) + (b_{i,\lambda}(\tau) - b_{f,\lambda}(\tau)) \lambda_t + (b_{i,\xi}(\tau) - b_{f,\xi}(\tau)) \xi_t \right].$$

Our view that the LIBOR-OIS spread directly reflects disaster risk is novel, but not inconsistent with the existing view on the source of interbank risk. Prior studies typically decompose interbank risk (and hence the LIBOR-OIS spread) into a liquidity component and a pure credit component.<sup>10</sup> We do not make such a distinction; we study the possibility of extreme tail events implied by the total risk of the interbank market, regardless of where it originates from. Modeling these market phenomena separately is beyond the scope of our paper. Instead, we simply capture the risk of such an economic downturn using disaster risk.

We also note that the fluctuations in the LIBOR-OIS spread are purely systematic in our framework, as they are driven by the risk of economic disasters. One might argue that this spread can also be influenced by bank-specific shocks. Granted, the LIBOR is calculated empirically using input data from only about a dozen contributor banks. However, they are large and systemically important banks; significant shocks to these banks cannot be purely idiosyncratic, considering their critical roles in the intricately intertwined banking system.

It is worth highlighting that we do not assume the yield on Treasury securities (simply, Treasury rate) to be our benchmark interest rate for riskless discounting; we choose the OIS rate instead, which is a conventional market proxy for the risk-free interest rate. The recent literature has documented that Treasury securities carry a convenience yield, derived from their special role as safe/liquid assets (e.g., Krishnamurthy and Vissing-Jorgensen, 2012).

---

<sup>10</sup>See, for example, Michaud and Upper (2008), Taylor and Williams (2009), Acharya and Skeie (2011), Filipović and Trolle (2013), and McAndrews, Sarkar, and Wang (2017).

This implies that the Treasury rate can go even below the true risk-free rate. Consistently, we define the  $\tau$ -maturity Treasury rate  $y_{g,t}^{(\tau)}$  as

$$y_{g,t}^{(\tau)} = y_{f,t}^{(\tau)} - y_{x,t}^{(\tau)},$$

where  $y_{x,t}^{(\tau)}$  represents the Treasury convenience yield, typically proxied by the OIS-Treasury spread.

In fact, the OIS-Treasury spread is on average positive in the data, supporting the presence of a convenience yield from holding Treasury securities. Nevertheless, the data reveals that this spread occasionally turns negative, most notably during the COVID-19 crisis (e.g., He, Nagel, and Song, 2022). To capture these properties in reduced form, we assume that the Treasury convenience yield is driven by an instantaneous convenience rate  $x_t$ , which follows a mean-reverting Gaussian process:

$$dx_t = \kappa_x(\bar{x} - x_t)dt + \sigma_x dB_{x,t}.$$

The standard Brownian motion  $B_{x,t}$  is assumed to be independent of other Brownian and Poisson shocks. Under this setup, the  $\tau$ -maturity convenience yield  $y_{x,t}^{(\tau)}$  is derived as

$$y_{x,t}^{(\tau)} = \frac{1}{\tau} \log \mathbb{E}_t \left[ e^{\int_t^{t+\tau} x_u du} \right] = -\frac{1}{\tau} \left[ a_x(\tau) + b_x(\tau)x_t \right], \quad (8)$$

where the expressions for the deterministic functions  $a_x$  and  $b_x$  are provided in Appendix A.2.

With the Treasury convenience, the spread between the LIBOR and the Treasury rate,

the so-called TED spread, becomes a function of  $(\lambda_t, \xi_t)$  as well as  $x_t$ :

$$\text{TED}_t^{(\tau)} = -\frac{1}{\tau} \left[ (a_i(\tau) - a_f(\tau) + a_x(\tau)) + (b_{i,\lambda}(\tau) - b_{f,\lambda}(\tau)) \lambda_t + (b_{i,\xi}(\tau) - b_{f,\xi}(\tau)) \xi_t + b_x(\tau) x_t \right].$$

This suggests that while the TED spread is still a meaningful indicator of disaster risk, its signal is relatively less clear than the LIBOR-OIS spread due to the added complexity introduced by the convenience factor  $x_t$ .

## 2.4 Options on interbank rates

In this section, we introduce derivative contracts called caps and swaptions whose payoffs depend on future interbank rates. When discussing their payoffs and pricing, it is convenient to introduce the following notation:

$$P_i(t, t + \tau) = \exp \left[ -\tau \cdot y_{i,t}^{(\tau)} \right].$$

In other words,  $P_i(t, t + \tau)$  represents the time- $t$  value of \$1 zero-coupon interbank lending maturing at time  $t + \tau$ . Additionally, we need the expression for the LIBOR in the model. Recall that the LIBOR is a simple interest rate and, therefore, is not exactly the same as the continuously compounded rate  $y_{i,t}^{(\tau)}$ . We can convert between the two interest rates using the following relation:

$$y_{i,t}^{(\tau)} = \frac{1}{\tau} \log \left[ 1 + \tau \text{LIBOR}_t^{(\tau)} \right], \text{ or equivalently, } \text{LIBOR}_t^{(\tau)} = \frac{1}{\tau} \left[ \exp \left( \tau \cdot y_{i,t}^{(\tau)} \right) - 1 \right].$$



An interest rate cap consists of a series of caplets that mature every 6 months.<sup>11</sup> Specifically, the first caplet matures 6 months from today, and the last caplet matures 6 months prior to the cap maturity date. Let  $T$  denote the time to maturity of a cap from today (time  $t$ ), and  $K$  denote its strike interest rate. For notational convenience, we define  $\Delta = 0.5$  and  $t_j = t + \Delta j$ .

The  $j$ -th caplet provides the holder of the cap with the right, not the obligation, to borrow a dollar at the rate of  $K$  between times  $t_j$  and  $t_{j+1}$ . If the future 6-month LIBOR at time  $t_j$  is higher than the strike  $K$ , this caplet is exercised and the holder borrows a dollar at the lower-than-the-fair interest rate. That is, the payoff from exercising the caplet is  $\Delta \times (\text{LIBOR}_{t_j}^{(0.5)} - K)$ . This payoff occurs at time  $t_{j+1}$  because the interest payment is made at the end of the borrowing period.

Since the cap is a collection of a  $m_T = (\frac{T}{\Delta} - 1)$  number of caplets, the time- $t$  cap value is calculated as

$$V_{\text{cap}}^{(T)}(t, K) = \sum_{j=1}^{m_T} \mathbb{E}_t^Q \left[ \exp \left( - \int_t^{t_{j+1}} r_s ds \right) \left[ \Delta \times (\text{LIBOR}_{t_j}^{(0.5)} - K) \right]^+ \right], \quad (9)$$

where  $\mathbb{Q}$  represents the risk-neutral measure (see Appendix A.1). In Appendix A.3, we demonstrate that equation (9) can be computed using the transform analysis of Duffie, Pan, and Singleton (2000).

An interest rate swaption grants the holder the right to enter into an interest rate swap (IRS). There are two types of swaptions. When exercised, a payer swaption delivers an IRS

---

<sup>11</sup>More precisely, a conventional cap contract traded in the market is a collection of caplets that mature every 3 months. As documented by Longstaff, Santa-Clara, and Schwartz (2001), assuming semi-annually spaced caplets for computational convenience is innocuous, generating a negligible difference when it comes to Black-implied volatilities.

where the holder pays the fixed leg and receives the LIBOR-based floating leg (a payer IRS); a receiver swaption delivers an IRS where the holder receives the fixed leg and pays the LIBOR-based floating leg (a receiver IRS). We now define  $T$  as the time to maturity of payer and receiver swaptions. Let  $K$  denote their strike interest rate. The tenor of the IRS at the maturity of the swaptions is denoted as  $\bar{T}$ . Under this notation, our swaptions of interest are often referred to as  $T$ -into- $\bar{T}$  swaptions.

The payer swaption is exercised if the future  $\bar{T}$ -maturity swap rate at time  $t + T$  is larger than the strike  $K$ . In this case, the holder enters into a payer IRS contract and makes a profit by exchanging the fixed rate  $K$  (which is lower than the fair swap rate) for the floating rate. The pricing relation implies that the time- $t$  payer swaption value is calculated by

$$V_{\text{payer}}^{(T, \bar{T})}(t, K) = \mathbb{E}_t^Q \left[ \exp \left( - \int_t^{t+T} r_s ds \right) \left[ V_{\text{floating}}^{(\bar{T})}(t + T, K) - V_{\text{fixed}}^{(\bar{T})}(t + T, K) \right]^+ \right], \quad (10)$$

where the value of the payer IRS delivered at option expiry, if exercised, is simply the difference between its floating leg  $V_{\text{floating}}^{(\bar{T})}(t + T, K)$  and its fixed leg  $V_{\text{fixed}}^{(\bar{T})}(t + T, K)$ . Similarly, the receiver swaption is exercised if the future  $\bar{T}$ -maturity swap rate at time  $t + T$  is smaller than the strike  $K$ . The time- $t$  receiver swaption value is expressed as

$$V_{\text{receiver}}^{(T, \bar{T})}(t, K) = \mathbb{E}_t^Q \left[ \exp \left( - \int_t^{t+T} r_s ds \right) \left[ V_{\text{fixed}}^{(\bar{T})}(t + T, K) - V_{\text{floating}}^{(\bar{T})}(t + T, K) \right]^+ \right]. \quad (11)$$

Traditionally, the industry norm was to calculate both the floating and fixed legs of an IRS based on LIBOR-swap discounting. However, the global financial crisis cast doubt on the validity of LIBOR-swap discounting. Going through the Lehman failure and the subsequent

credit crunch that led to a sharp rise in LIBOR, the market migrated to OIS discounting, which is now the new norm for derivative pricing (Hull and White, 2015). While our sample period includes both pre-crisis and post-crisis periods, we believe that OIS discounting is theoretically more suitable, especially given that most derivative trades require margins and are heavily collateralized.

However, when it comes to tractability, there is a significant benefit of using LIBOR-swap discounting: it always puts the floating leg at par because the floating coupons and their discount rates are both based on future LIBOR rates. As a result, the IRS pricing reduces to computing the fixed leg  $V_{\text{fixed}}^{(\bar{T})}(t+T, K)$ , which is equivalent to the value of a coupon bond with the (annualized) coupon rate of  $K$ :

$$V_{\text{fixed}}^{(\bar{T})}(t+T, K) = \Delta \left[ K \sum_{j=1}^{\bar{T}/\Delta} P_i(t+T, t+T+j\Delta) \right] + P_i(t+T, t+T+\bar{T}). \quad (12)$$

For analytical tractability, we opt for the simplifying assumption that the future IRS contract, delivered at option expiry, is valued using LIBOR-swap discounting.<sup>12</sup> Then, equation (12) suggests that interest rate swaptions can essentially be viewed as options on a coupon bond. Due to coupon payments, the expression for the coupon bond price contains multiple terms, which makes it impossible to calculate the expectations in equations (10) and (11) using the semi-analytic approach of Duffie, Pan, and Singleton (2000). We adopt the stochastic duration method implemented by Trolle and Schwartz (2009), which enables us to accurately approximate the price of a coupon bond option by a constant multiplication of the

---

<sup>12</sup>Under OIS discounting, the floating leg of a LIBOR-based IRS is no longer at par and is worth more than 1. Consequently,  $V_{\text{floating}}^{(\bar{T})}(t+T, K)$  remains in the swaption pricing formula. This term makes it virtually impossible to obtain a semi-analytical solution. Handling the fixed leg  $V_{\text{fixed}}^{(\bar{T})}(t+T, K)$  alone already requires an approximation called the stochastic duration method due to numerous coupon terms; adding floating coupons further complicates the pricing formula to an extreme level.

price of a zero-coupon bond option (see, e.g., Wei, 1997; Munk, 1999). We provide a detailed description of the swaption pricing procedure in Appendix A.3.

## 3 Estimation

### 3.1 Data

Our data sample consists of the following variables: interbank rates, OIS rates, Treasury rates, Black-implied volatilities for caps and swaptions, expected inflation, and real consumption per capita. All variables are sampled at the monthly frequency at the end of each month, from February 2002 to December 2019.

Interbank rates consist of 3-, 6-, and 12-month LIBOR rates as well as 2-, 3-, and 5-year swap rates, all of which are downloaded from Bloomberg.<sup>13</sup> We also collect OIS rates from Bloomberg and Treasury rates from FRED for the same maturities. To make the data comparable with the model-implied interest rates, we need to convert the three types of interest rate term structures into continuously compounded zero curves. To do so, we use linear interpolation to construct par curves with maturities ranging from 6 months to 5 years with 6-month intervals. From these interpolated par curves, we extract smooth forward rate curves and, in turn, zero-coupon yield curves via the Nelson and Siegel (1987) parameterization. Summary statistics for these interest rates are reported in Panels A, B, and C of Table 1.

Note that our analysis relies on interest rates with maturities of up to 5 years, despite their

---

<sup>13</sup>On March 5, 2021, the ICE Benchmark Administration Limited announced the complete discontinuation of the publication of USD LIBOR effective June 30, 2023. The crucial role of USD LIBOR as a benchmark interest rate will be largely taken over by the secured overnight financing rate (SOFR). See Jermann (2019), Jermann (2020a), and Klingler and Syrstad (2021) for further discussion about the transition from USD LIBOR to SOFR.

	Mean	SD	Min	Median	Max	AR1
<b>Panel A: Treasury rate</b>						
3M	1.32	1.51	0.00	0.95	5.13	0.993
6M	1.43	1.53	0.03	1.01	5.17	0.994
1Y	1.55	1.48	0.11	1.23	5.14	0.993
2Y	1.74	1.40	0.15	1.37	5.09	0.988
3Y	2.00	1.31	0.32	1.61	5.06	0.984
5Y	2.44	1.20	0.57	2.21	5.03	0.976
<b>Panel B: OIS rate</b>						
3M	1.45	1.59	0.08	1.00	5.35	0.995
6M	1.48	1.59	0.08	1.04	5.41	0.995
1Y	1.59	1.58	0.10	1.17	5.50	0.993
2Y	1.80	1.53	0.12	1.35	5.45	0.989
3Y	2.07	1.47	0.23	1.61	5.44	0.986
5Y	2.49	1.40	0.48	2.17	5.47	0.981
<b>Panel C: Interbank rate</b>						
3M	1.71	1.60	0.22	1.18	5.58	0.992
6M	1.85	1.54	0.32	1.34	5.51	0.993
1Y	2.07	1.42	0.54	1.64	5.56	0.991
2Y	2.10	1.46	0.39	1.66	5.55	0.988
3Y	2.31	1.44	0.44	1.89	5.55	0.985
5Y	2.76	1.34	0.75	2.56	5.56	0.979
<b>Panel D: Cap IV</b>						
2Y	49.65	25.10	12.18	50.52	102.70	0.969
3Y	46.41	21.56	13.43	46.30	93.22	0.964
4Y	43.43	18.63	13.99	43.03	82.59	0.958
5Y	40.26	15.97	14.26	39.80	77.47	0.954
<b>Panel E: Swaption IV</b>						
1-into-4	36.57	12.88	13.20	37.20	75.22	0.924
2-into-3	34.88	12.01	14.10	34.09	70.75	0.932
3-into-2	33.47	11.67	14.55	32.28	67.86	0.936
4-into-1	32.16	11.35	14.60	30.50	69.33	0.931

**Table 1: Summary statistics.** This table reports the mean, standard deviation, minimum, median, maximum, and first-order autoregressive coefficient (AR1) of continuously-compounded zero-coupon Treasury rates (Panel A), OIS rates (Panel B), and interbank rates (Panel C), as well as cap and swaption implied volatilities (Panels D and E). All values are expressed in percentage terms, except for the AR1, which is unitless.

availability of up to 30 years. This is our intentional choice, as long-term interest rates are potentially subject to some frictions that are beyond our model. In particular, since the 2008 financial crisis, the 30-year swap rate has maintained a lower level than the 30-year Treasury rate, which poses a puzzle. This phenomenon is not just seen in the 30-year maturity: we frequently observe a negative swap spread for any long-term maturity between 5 years and 30 years. Klingler and Sundaresan (2019) argue that negative swap spreads reflect underfunded

pension plans’ increased demand for duration hedging with long-term swaps. Even without such explicit demand effects, Jermann (2020b) shows that negative swap spreads can be justified via limits to arbitrage associated with frictions for holding long-term Treasuries. Rather than incorporating extra frictions into our model, we keep our model simple and focus on short- and mid-term interest rates.

We download the pricing data on caps and swaptions from Bloomberg.<sup>14</sup> Caps and swaptions are typically quoted in terms of Black-implied volatilities. For each market price, the corresponding Black-implied volatility is found by backsolving the volatility term in the Black (1976) model. Caps and swaptions in our sample are at-the-money forward (ATMF), meaning that the strike price of each option is equal to the current forward price of the underlying. Specifically, the strike price of a  $T$ -maturity ATMF cap is the  $T$ -maturity swap rate. The strike price of a  $T$ -into- $\bar{T}$  ATMF swaption is the forward swap rate between the option expiry ( $T$  years from today) and the underlying swap expiry ( $T + \bar{T}$  years from today). Panels D and E of Table 1 present summary statistics for cap and swaption implied volatilities.

The data on expected inflation is from the Blue Chip Economic Indicators survey. This dataset provides the forecasts of inflation for the current calendar year and the next calendar year. For each month, we calculate a proxy for the 1-year-ahead expected inflation by calculating the weighted average between the two forecasts. Lastly, the monthly time series of real consumption per capita is downloaded from FRED.

---

<sup>14</sup>There are multiple sources for caps and swaptions data on Bloomberg. We mainly use the sources “CMPN” for caps and “BBIR” for swaptions, which provide the Black-implied volatilities calculated based on LIBOR-swap discounting.

### 3.2 Unscented Kalman filter and maximum likelihood estimation

From the data described in Section 3.1, we filter the time series of the latent processes  $(\lambda_t, \xi_t, \mu_t, x_t)$  using the unscented Kalman filter and estimate the model parameters via maximum likelihood estimation (MLE). In this section, we detail our model estimation procedure.

Estimating our model is computationally challenging. In each iteration of the MLE procedure, we need to evaluate the log-likelihood function. Due to cap/swaption pricing, this requires numerically solving the system of complex-valued ordinary differential equations of Duffie, Pan, and Singleton (2000) several times. Furthermore, we have a large number of parameters to be estimated. Evidently, estimating all of these parameters all at once in a single MLE is highly time-consuming.

To alleviate the computational burden, we first separately estimate the parameters  $\kappa_q$ ,  $\bar{q}$ , and  $\sigma_q$ , which govern the normal-time dynamics of expected inflation. This is possible because a consumption disaster is absent during our sample period, implying that the observed time series of expected inflation was completely driven by these three parameters. Specifically,  $\kappa_q$ ,  $\bar{q}$ , and  $\sigma_q$  are estimated by maximizing the log-likelihood of the expected inflation time series, conditional on no disasters. We also set  $\bar{\mu}$  to be 1.05%, which is the average real consumption growth during our sample period.

We further reduce the dimension of our parameter space by putting a restriction on the value of  $\delta_0$ . Taking expectations on both sides of equation (5) results in:

$$\mathbb{E}[r] = \delta_0 + \delta_\lambda \mathbb{E}[\lambda] + \delta_\xi \mathbb{E}[\xi] + \delta_\mu \mathbb{E}[\mu] + \delta_q \mathbb{E}[q].$$

Here, we proxy the unconditional mean of the short rate ( $\mathbb{E}[r]$ ) by the average 1-week OIS

rate ( $\hat{\mathbb{E}}[r]$ ) from Bloomberg. Then, the value of  $\delta_0$  is given by

$$\delta_0 = \hat{\mathbb{E}}[r] - \delta_\lambda \bar{\xi} - \delta_\xi \bar{\xi} - \delta_\mu \bar{\mu} - \delta_q \hat{\mathbb{E}}[q],$$

where  $\hat{\mathbb{E}}[q]$  is the average expected inflation during our sample period.

Moreover, we set  $\bar{\xi}$  to be 2.86%, which is the average probability of consumption disasters across OECD countries, according to Barro and Ursúa (2008). We also construct the empirical distributions of  $Z_{C,t}$  and  $Z_{q,t}$  by compiling consumption declines and inflation rates during historical consumption disasters from the Barro-Ursua dataset.<sup>15</sup> Lastly, we assume  $Z_{L,t} = Z_{C,t}$ : the more severe the interbank market failure, the more severe the consumption disaster.<sup>16</sup>

As a result, we are left with 20 parameters to be estimated within the main MLE procedure:

$$\Theta = [\kappa_\mu, \sigma_\mu, \sigma_C, \kappa_\xi, \sigma_\xi, \kappa_\lambda, \sigma_\lambda, \kappa_x, \sigma_x, \bar{x}, \bar{p}, \delta_\lambda, \delta_\xi, \delta_\mu, \delta_q, \theta_\lambda, \theta_\xi, \theta_\mu, \theta_q, \theta_N],$$

besides three extra parameters concerning measurement errors (described below). We derive the likelihood function  $\mathcal{L}$  under the assumption that we observe the following: (i) LIBOR-OIS spreads and TED spreads with 3-, 6-, 12-month maturities, (ii) interbank rates, OIS rates, and Treasury rates with 3-, 6-, 12-month, 2-, 3-, 5-year maturities, (iii) 2-, 3-, 4-, 5-year cap implied volatilities, (iv) 1-into-4, 2-into-3, 3-into-2, 4-into-1 swaption implied volatilities, and (v) real consumption growth. For notational simplicity, we let  $Y_t$  denote the vector of all these

---

<sup>15</sup>The Barro-Ursua dataset contains a few extreme hyperinflation events, such as the hyperinflation of Weimar Germany in the 1920s when the inflation rate exceeded 3,000%. Given that the number of historical consumption disasters is only 89, such extreme outliers completely dominate the moment generating function of  $Z_{q,t}$ . Thus, we exclude the observations that fall more than 3 times the interquartile range above the third quartile. No observations fall more than 3 times the interquartile range below the first quartile.

<sup>16</sup>We can relax this assumption by setting  $Z_{L,t} = kZ_{C,t}$  and estimating  $k$  directly. However, in this case, the coefficient  $k$  is not well identified separately from  $\bar{p}$ ; an increase (decrease) in  $k$  can be compensated by a decrease (increase) in  $\bar{p}$  or vice versa.



observations at time  $t$ .

To construct the likelihood function  $\mathcal{L}$ , it suffices to derive the transition density of  $Y_t$ . Specifically, we define  $\mathcal{L}_t$  as the likelihood of observing  $Y_t$  conditional on  $Y_{t-\Delta t}$ :

$$\mathcal{L}_t = \mathbb{P}(Y_t | Y_{t-\Delta t}; \Theta),$$

where  $\Delta t = 1/12$  represents monthly time intervals between observations. Not only does this transition density depend on the observable state variable  $q_t$ , but it also relies on the four latent variables  $\lambda_t$ ,  $\xi_t$ ,  $\mu_t$ , and  $x_t$ .

In order to solve this filtering problem, we specify the state equation and the measurement equation in the state-space representation of our model. The state equation describes the dynamics of a latent state vector  $S_t = [\lambda_t, \xi_t, \mu_t, x_t]^\top$ . There are two ways to map the continuous-time dynamics of  $S_t$  into the discrete-time state equation. The first approach applies the Euler discretization to  $\lambda_t$ ,  $\xi_t$ ,  $\mu_t$ , and  $x_t$  and then finds the discrete-time relation between  $S_t$  and  $S_{t-\Delta t}$ . In contrast, the second approach finds the exact relation between  $S_t$  and  $S_{t-\Delta t}$  without any approximation and then discretizes the resulting relation. We adopt the latter approach following Chen and Scott (2003), as it better captures the square-root diffusions of the first two latent processes. Consequently, we arrive at the following linear state equation:

$$S_t = \eta + \Psi S_{t-\Delta t} + \epsilon_t, \quad \text{where } \mathbb{E}_{t-\Delta t} [\epsilon_t \epsilon_t^\top] = \Omega_{t-\Delta t}. \quad (13)$$

We provide the expressions for four-dimensional vector  $\eta$ ,  $4 \times 4$  matrix  $\Psi$ , and  $4 \times 4$  time-varying covariance matrix  $\Omega$  in the Internet Appendix. Since  $\epsilon_t$  is non-normal, we approximate it by a normal distribution with the same covariance matrix. Prior studies document that

this approximation is innocuous.<sup>17</sup>

Now, we turn to the measurement equation. We assume that  $Y_t$  is observed with a vector of measurement errors  $e_t$ :

$$Y_t = h(S_t, q_t) + e_t, \quad \text{where } \mathbb{E}_{t-\Delta t} [e_t e_t^\top] = Q.$$

Note that  $h$  is a vector-valued function of the state variables, which generates the model counterparts of the data. The mean-zero random vector  $e_t$  is normally distributed with covariance matrix  $Q$ . For parsimony, all measurement errors are assumed to be independent of one another, making the off-diagonal entries of  $Q$  zero. As for the diagonal entries, we assume that the standard deviations of the measurement errors are identical for the interest rate spreads ( $\sigma_{SP}$ ), for the interest rates ( $\sigma_{ITR}$ ), and for the Black-implied volatilities ( $\sigma_{OPT}$ ). The measurement equation clearly suggests that the linear Kalman filter cannot be used in our estimation. This is because  $h$  is not a linear function: cap/swaption prices as well as their Black-implied volatilities are nonlinear in the state variables. Therefore, we apply the unscented Kalman filter, proposed by Wan and Van Der Merwe (2000). The Internet Appendix provides a detailed description of how the unscented Kalman filter is implemented under our setup.

In each iteration of the MLE procedure, we obtain not only the time series of the estimated latent variables  $\{\hat{\lambda}_t, \hat{\xi}_t, \hat{\mu}_t, \hat{x}_t\}$ , but also the time series of the transition densities  $\{\mathcal{L}_t\}$ . Let  $\{t_k\}_{k=1}^n$  denote monthly-spaced points in time when the data time series are observed. Then,

---

<sup>17</sup>See, for example, Duan and Simonato (1999), Duffee (1999), Chen and Scott (2003), Trolle and Schwartz (2009), and Filipović and Trolle (2013).

the log-likelihood function for the entire observations can finally be expressed as

$$\log \mathcal{L} = \sum_{k=1}^n \log \mathcal{L}_{t_k}.$$

We determine the parameter estimates by maximizing this log-likelihood function.

## 4 Estimation results and implications

### 4.1 Parameter estimates

Table 2 reports the values of our parameter estimates, along with their robust standard errors in parentheses. First of all, The estimated dynamics of consumption growth and expected inflation are economically sensible. During normal periods without disasters, consumption growth has a long-run mean ( $\bar{\mu}$ ) of 1.05% and a standard deviation ( $\sigma_C$ ) of 0.81%, broadly consistent with the first two moments of the observed consumption time series in our sample. The process of mean consumption growth  $\mu_t$  is not only persistent with  $\kappa_\mu = 0.7343$  but also quite volatile with  $\sigma_\mu = 0.37\%$ . The parameter values for expected inflation are also in line with its data time series: the long-run mean ( $\bar{q}$ ) is 2.12%, the conditional volatility ( $\sigma_q$ ) is 0.65%, and the monthly autocorrelation ( $e^{-\kappa_q \Delta t}$ ) is 0.96.<sup>18</sup>

Our main focus is on the model parameters that are associated with the dynamics of disaster risk. In our model, disaster risk has a two-factor structure with  $\lambda_t$  and  $\xi_t$ . While both processes are estimated to be highly persistent with low mean reversion speed ( $\kappa_\lambda = 0.4373$

---

<sup>18</sup>While expected inflation plays a crucial role in capturing the level of interest rates in our model, its omission is not impossible given that our model is reduced-form. In the Internet Appendix, we consider a nested case of our model without expected inflation and show that it is rejected based on a likelihood ratio test.

Consumption growth	Est. (SE)	$\kappa_\mu$ 0.7343 (0.0152)	$\sigma_\mu$ 0.0037 (0.0002)	$\sigma_C$ 0.0081 (0.0005)	$\bar{\mu}$ 0.0105	
Expected inflation	Est. (SE)	$\kappa_q$ 0.5239 (0.3153)	$\sigma_q$ 0.0065 (0.0011)	$\bar{q}$ 0.0212 (0.0028)		
Disaster risk	Est. (SE)	$\kappa_\xi$ 0.0446 (0.0071)	$\sigma_\xi$ 0.0204 (0.0002)	$\bar{\xi}$ 0.0286		
	Est. (SE)	$\kappa_\lambda$ 0.4373 (0.0130)	$\sigma_\lambda$ 0.1560 (0.0039)	$\bar{p}$ 0.9035 (0.0295)		
Convenience yield	Est. (SE)	$\kappa_x$ 0.8162 (0.1915)	$\sigma_x$ 0.0017 (0.0003)	$\bar{x}$ 0.0021 (0.0004)		
Short rate	Est. (SE)	$\delta_\lambda$ -0.1443 (0.0026)	$\delta_\xi$ -2.1572 (0.1160)	$\delta_q$ 0.4594 (0.0251)	$\delta_\mu$ 2.1835 (0.0356)	$\delta_0$ 0.0476
Market price of risk	Est. (SE)	$\theta_\lambda$ -0.1355 (0.0031)	$\theta_\xi$ -0.6377 (0.0589)	$\theta_q$ -3.6234 (0.0870)	$\theta_\mu$ 0.2696 (0.0139)	$\theta_N$ -0.1075 (0.0061)
Measurement errors	Est. (SE)	$\sigma_{SP}$ 0.0014 (0.0001)	$\sigma_{ITR}$ 0.0020 (0.0001)	$\sigma_{OPT}$ 0.0742 (0.0032)		

**Table 2: Parameter estimates.** This table reports the values of the model parameters estimated through the unscented Kalman filter/MLE procedure. The model consists of the following five state variables: real consumption ( $C_t$ ), mean consumption growth ( $\mu_t$ ), expected inflation ( $q_t$ ), instantaneous disaster intensity ( $\lambda_t$ ), and the long-run mean of disaster intensity ( $\xi_t$ ). We also report the dynamics of the instantaneous Treasury convenience rate ( $x_t$ ), the factor loadings on the short rate, the market prices of risk, and the standard deviations of measurement errors. Reported together in parentheses are robust standard errors.

and  $\kappa_\xi = 0.0446$ ),  $\lambda_t$  is relatively less persistent than  $\xi_t$ . This is intuitive because  $\lambda_t$  captures the short-run component of disaster risk, whereas  $\xi_t$  captures the long-run component. Consistent with this interpretation,  $\lambda_t$  exhibits a higher conditional volatility than  $\xi_t$  (i.e.,  $\sigma_\lambda > \sigma_\xi$ ). In Section 4.3, we further characterize the time variation in disaster risk by examining the filtered time series of  $\lambda_t$  and  $\xi_t$ . The conditional probability of interbank market failure given the occurrence of a disaster ( $\bar{p}$ ) is estimated as 0.9035, suggesting that the two types of extreme events are indeed likely to coincide.

We also report the estimated dynamics of the instantaneous convenience rate  $x_t$ . Relative to  $\lambda_t$  and  $\xi_t$ , the process for  $x_t$  is much less persistent with  $\kappa_x = 0.8162$ , which corresponds

to a monthly autocorrelation of 0.93. The long-run mean ( $\bar{x}$ ) is 0.21%, and the conditional volatility ( $\sigma_x$ ) is 0.17%. Given that the average 3-month Treasury rate is only about 1.32% over our sample period, the relative magnitude of the Treasury convenience yield is not small.

The estimated coefficients  $\delta_\lambda$ ,  $\delta_\xi$ ,  $\delta_q$ , and  $\delta_\mu$  in Table 2 show how the four state variables  $\lambda_t$ ,  $\xi_t$ ,  $q_t$ , and  $\mu_t$  affect the nominal short rate in our estimated model. We first observe that the factor loading on expected inflation is positive. This conforms to the economic intuition that expected inflation rises with nominal interest rates. While expected inflation is an important factor, empirical evidence suggests that a significant portion of the variation in the nominal short rate is still attributable to the variation in the real short rate (Haubrich, Pennacchi, and Ritchken, 2012). The table reports that the factor loading is positive for  $\mu_t$  but negative for  $\lambda_t$  and  $\xi_t$ . This is in accordance with the precautionary savings motive. Investors are inclined to save more to secure against future uncertainty when mean consumption growth declines or disaster risk rises, driving down real interest rates.

Additionally reported are the market prices of risk. The coefficients  $\theta_\lambda$ ,  $\theta_\xi$ , and  $\theta_q$  are negative, as investors dislike both horizons of disaster risk and inflation risk: investors' marginal utility, or equivalently, the pricing kernel in equation (4), rises when positive realizations of  $dB_{\lambda,t}$ ,  $dB_{\xi,t}$ , and  $dB_{q,t}$  raise  $\lambda_t$ ,  $\xi_t$ , and  $q_t$ , respectively. Similarly, Poisson shocks are also priced negatively with  $\theta_N < 0$ . Since  $e^{\theta_N Z_{C,t}}$  is larger than 1, the pricing kernel jumps up when a disaster occurs ( $dN_t = 1$ ). In contrast, the coefficient  $\theta_\mu$  is positive, as  $dB_{\mu,t}$  is a good economic shock that increases consumption growth. All in all, we conclude that the signs and magnitudes of the model parameters from our estimation align well with general economic intuition.

## 4.2 Model fit to interest rates, caps, and swaptions

We now investigate whether our estimated model is capable of producing a reasonable fit to the market data on interest rates, caps, and swaptions. Figure 1 first examines short-term interest rates by plotting the time series of the 3-month Treasury rate (Panel A), OIS rate (Panel B), interbank rate (Panel C), LIBOR-OIS spread (Panel D), TED spread (Panel E), and Treasury convenience yield (Panel F) in the data (solid blue lines) and in the model (dashed red lines).

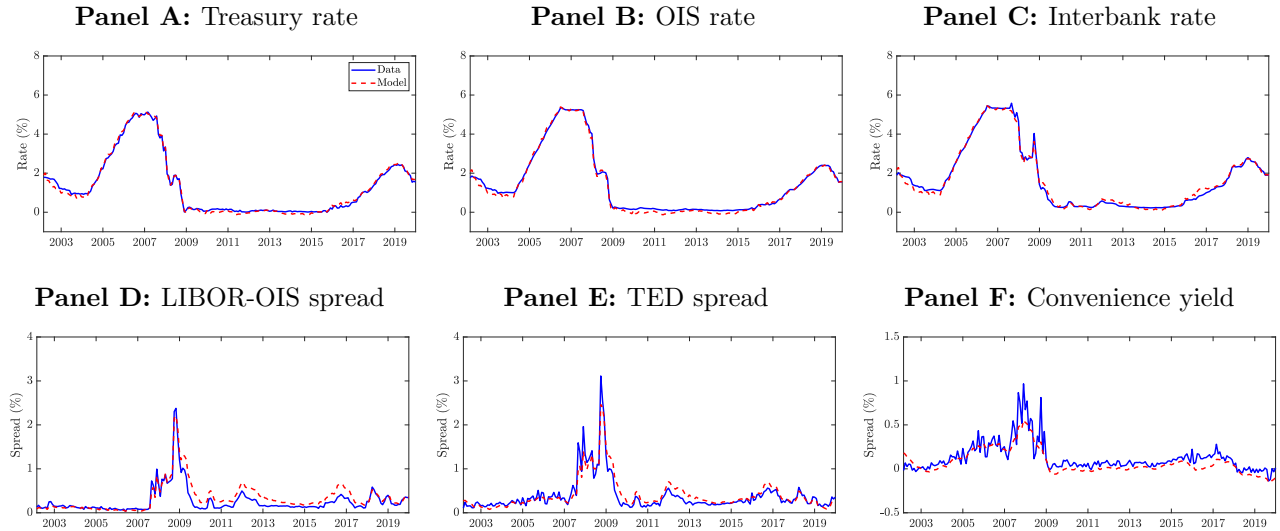


**Figure 1: 3-month interest rates and their spreads in the data and in the model.** This figure plots the time series of the 3-month Treasury rate (Panel A), OIS rate (Panel B), interbank rate (Panel C), LIBOR-OIS spread (Panel D), TED spread (Panel E), and Treasury convenience yield (Panel F) in the data and in the model, from February 2002 to December 2019. The solid blue lines represent the data, and the dashed red lines represent the model. All interest rates are calculated using continuously compounded zero rates and are expressed in percentage terms.

Panel A of Figure 1 shows that at the beginning of our data sample, the Treasury rate entered a steady downward trend up until 2004. During this time, the Federal Reserve lowered the federal funds rate from 6% to 1%, as investors faced high economic and financial uncertainty stemming from the 2001 recession, September 11 attacks, and Afghanistan War. This period of expansionary monetary policy was followed by a 3-year period of contractionary

monetary policy due to a housing market bubble and high inflation, causing the Treasury rate to gradually increase. From 2007, the Treasury rate began to rapidly decline again when the economy was hit by the subprime mortgage crisis and eventually reached a level close to zero. Since then, the Treasury rate maintained a very low level until the Federal Reserve started raising interest rates in 2015.

The 3-month OIS rate in Panel B and the 3-month interbank rate in Panel C also exhibit similar time series patterns compared to the 3-month Treasury rate, although their magnitudes are generally larger. However, a distinctive pattern is observed around September 2008 when Lehman Brothers filed for bankruptcy. In contrast to the other two rates, the interbank rate sharply increased, reflecting a serious risk of a potential systemic meltdown in financial markets. This event is more noticeable from the time series of the LIBOR-OIS spread in Panel D and that of the TED spread in Panel E. While the LIBOR-OIS spread stayed at a high level between 2007 and 2009 during the Great Recession period, an exceptionally high value of roughly 2.4% was seen in September 2008. Fluctuations in the TED spread are more magnified. As can be seen in Panel F, the 3-month Treasury convenience yield shot up to about 1% and remained high as investors hoarded Treasury securities (flight-to-safety/liquidity). As a result, the TED spread, which is the sum of the LIBOR-OIS spread and the Treasury convenience yield, sharply went up, even beyond 3%.

From the six panels of Figure 1, we find that our model effectively accounts for the patterns of the three types of interest rates as well as their spreads. The dashed red lines that represent the model-implied time series closely resemble the solid blue lines that represent the data time series, peaking and dipping at similar points in time. This holds true for longer-maturity interest rates as well. In Figure 2, the model-implied Treasury rates, OIS rates, and interbank

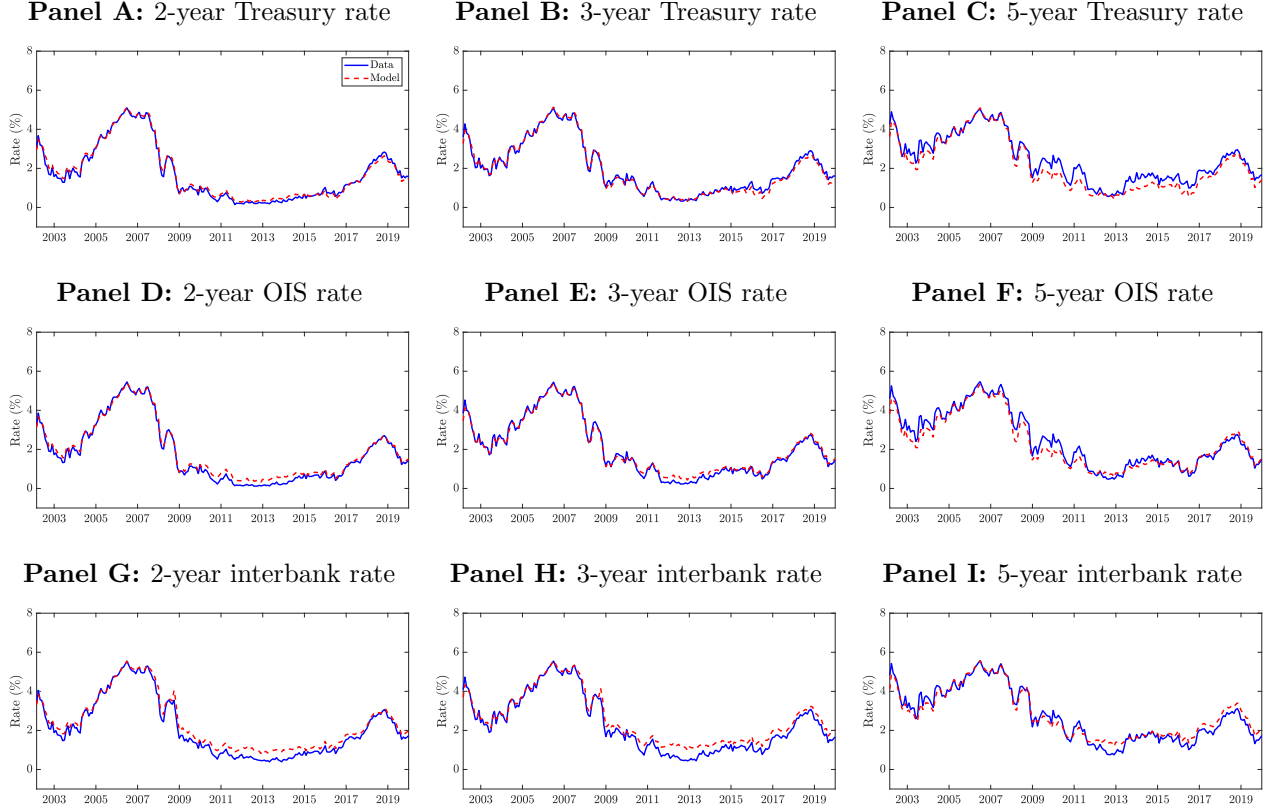


**Figure 2: Interest rates in the data and in the model.** This figure depicts the time series of the Treasury rates (Panels A, B, and C), OIS rates (Panels D, E, and F), and interbank rates (Panels G, H, and I) with 2-, 3-, and 5-year maturities in the data and in the model, from February 2002 to December 2019. The solid blue lines represent the data, and the dashed red lines represent the model. All values are expressed in percentage terms.

rates with 2-, 3-, and 5-year maturities closely track their data counterparts. More formally, Panel A of Table 3 reports three measures of empirical performance: mean error (ME), mean absolute error (MAE), and mean relative error (MRE). The pricing errors for interest rates, while slightly increasing with maturity, are small across the board. For instance, the MAEs range from 0.05% (6 months) to 0.25% (5 years), confirming that the model captures the interest rate data fairly well.

We now turn to caps and swaptions. Panels A, B, and C of Figure 3 present the time series of the Black-implied volatilities for the 2-, 3-, and 5-year caps, while Panels D, E, and F present those for the 1-into-4, 2-into-3, and 4-into-1 swaptions. In each panel, the solid blue



<b>Panel A: Mean pricing errors</b>							
		3M	6M	1Y	2Y	3Y	5Y
Interest rates	ME	0.0003	0.0002	-0.0001	-0.0014	-0.0009	0.0013
	MAE	0.0011	0.0005	0.0010	0.0017	0.0016	0.0025
	MRE	0.0190	0.0135	-0.0081	-0.0721	-0.0374	0.0532
		2Y	3Y	4Y	5Y		
Cap IVs	ME	-0.0369	0.0023	0.0146	0.0094		
	MAE	0.1293	0.0805	0.0532	0.0466		
	MRE	-0.0743	0.0049	0.0335	0.0234		
		1-into-4	2-into-3	3-into-2	4-into-1		
Swaption IVs	ME	0.0634	0.0553	0.0405	0.0184		
	MAE	0.0702	0.0593	0.0516	0.0489		
	MRE	0.1734	0.1585	0.1211	0.0573		
<b>Panel B: Regressions of data on model-implied values</b>							
		3M	6M	1Y	2Y	3Y	5Y
Interest rates	Coef.	0.98	1.00	1.01	1.04	1.02	0.98
	<i>t</i> -stat	[193.74]	[455.85]	[230.11]	[143.57]	[111.10]	[74.76]
	$R^2$ (%)	99.34	99.80	99.35	98.92	98.05	95.42
		2Y	3Y	4Y	5Y		
Cap IVs	Coef.	0.74	0.84	0.87	0.83		
	<i>t</i> -stat	[13.91]	[19.22]	[28.95]	[30.36]		
	$R^2$ (%)	71.67	81.57	89.07	91.58		
		1-into-4	2-into-3	3-into-2	4-into-1		
Swaption IVs	Coef.	0.82	0.84	0.83	0.77		
	<i>t</i> -stat	[15.32]	[17.87]	[17.08]	[13.88]		
	$R^2$ (%)	79.73	87.74	87.86	84.83		

**Table 3: Pricing errors.** This table evaluates the empirical performance of our model. Panel A reports three measures of mean pricing errors: mean error (ME), mean absolute error (MAE), and mean relative error (MRE), averaged by security type (interest rates, cap implied volatilities, and swaption implied volatilities) and maturity. Panel B presents regressions of each data series on its corresponding model-implied series and reports the resulting slope coefficients and  $R^2$  values. The *t*-statistics, shown in brackets, are computed using the Newey and West (1987) method with four lags.

line denotes the data, and the dashed red line denotes the model. The figure shows that our model's fit to the data is decent but not perfect. As reported in Panel A of Table 3, the MAEs of cap and swaption implied volatilities range between 5% and 8%, except for the 2-year cap, which has an MAE of 13%. It is not surprising that our model cannot accurately match every cap or swaption. Prior studies document that it is challenging to jointly account for the pricing of caps and swaptions in crisis periods, even with flexible statistical models featuring several latent processes (Longstaff, Santa-Clara, and Schwartz, 2001; Han, 2007; Trolle and

Schwartz, 2009).<sup>19</sup> Our objective is not to fit the data perfectly. Rather, we attempt to characterize time-varying disaster risk by exploiting the information contained in interbank rates and their options. Instead of adding more factors to improve the fit, we choose to keep our model simple and parsimonious. For our purposes, we believe that our simple economic model does a reasonably good job of capturing the data overall.<sup>20</sup>

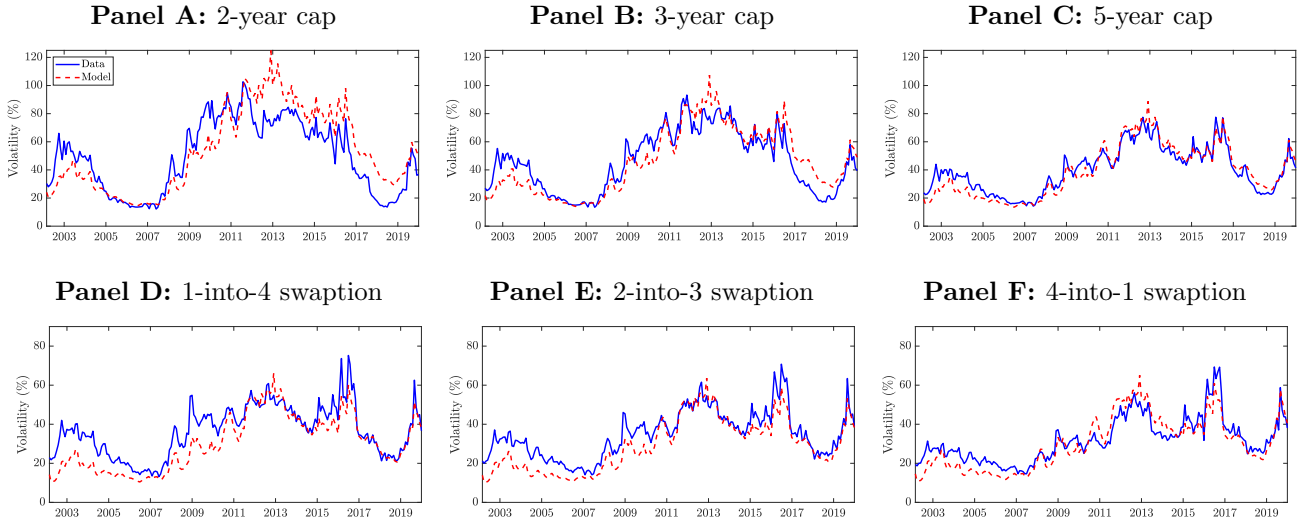


**Figure 3: Black-implied volatilities in the data and in the model.** This figure presents the time series of the Black-implied volatilities for the 2-, 3-, and 5-year caps (Panels A, B, and C) and those for the 1-into-4, 2-into-3, and 4-into-1 swaptions (Panels D, E, and F) in the data and in the model. The sample period is from February 2002 to December 2019. The solid blue lines represent the data, and the dashed red lines represent the model. All values are expressed in percentage terms.

Panel B of Table 3 further assesses model fit by regressing each data series on its corresponding model-implied series (see, e.g., Bakshi, Crosby, Gao, and Hansen, 2023). The resulting slope coefficients are reported alongside the  $R^2$  values. If the model accurately captures the time-series variation in the data, the estimated slope coefficients should be close to one and the regression should yield a high  $R^2$ . The panel shows that slope coefficients for in-

<sup>19</sup>Related, Bakshi, Crosby, Gao, and Hansen (2023) explain Treasury yields and option prices by adopting several latent variables, including both spanned and unspanned factors.

<sup>20</sup>Directly interpreting the magnitude and the time series variation of Black-implied volatilities for caps and swaptions may not be as intuitive because they represent yield volatilities, rather than bond price volatilities. In the Internet Appendix, we examine our model fit when Black-implied volatilities are converted into their equivalent bond price volatilities.

terest rates are indeed close to one, ranging from 0.98 to 1.04, and are statistically significant with extremely high  $R^2$  values between 95.42% and 99.80%. For cap and swaption implied volatilities, the model yields somewhat lower but still substantial slope coefficients ranging from 0.74 to 0.87, with  $R^2$  values between 71.67% and 91.58%. Taken together, these results demonstrate that our estimated model provides a good fit to the data.

### 4.3 Characterizing time-varying disaster risk

Our estimation procedure enables us to characterize the time variation in disaster risk via the unscented Kalman filter. Figure 4 presents the filtered time series of the short-run disaster risk component  $\lambda_t$  (solid blue line) and the long-run disaster risk component  $\xi_t$  (dashed red line), along with their summary statistics.<sup>21</sup>

The figure clearly shows that the instantaneous disaster risk  $\lambda_t$  is much more volatile than its time-varying mean  $\xi_t$ . Since  $\lambda_t$  is highly persistent, it sometimes significantly deviates from its mean value of 2.86% for extended periods of time. While  $\lambda_t$  hovered around a low level below 1% between 2002 and 2006, it abruptly increased to an extremely high level at the onset of the subprime mortgage crisis in 2007. During the subsequent 2-year period of severe economic downturns and financial market turmoil,  $\lambda_t$  persisted at levels above 4%. When Lehman Brothers declared bankruptcy in September 2008,  $\lambda_t$  reached its highest value, exceeding 11%. After the crisis, the level of  $\lambda_t$  came back to a normal level, but we still can see some small peaks that are associated with economic and financial uncertainty, such as in the European sovereign debt crisis.<sup>22</sup> The standard deviation of  $\lambda_t$  is 1.65% during our

---

<sup>21</sup>The filtered time series and summary statistics of the other two latent variables  $x_t$  and  $\mu_t$  are reported in the Internet Appendix.

<sup>22</sup>The Internet Appendix extends the data to December 2020 and examines how disaster risk evolved during the COVID-19 pandemic crisis. It shows that the short-run component  $\lambda_t$  jumped up during the peak of the

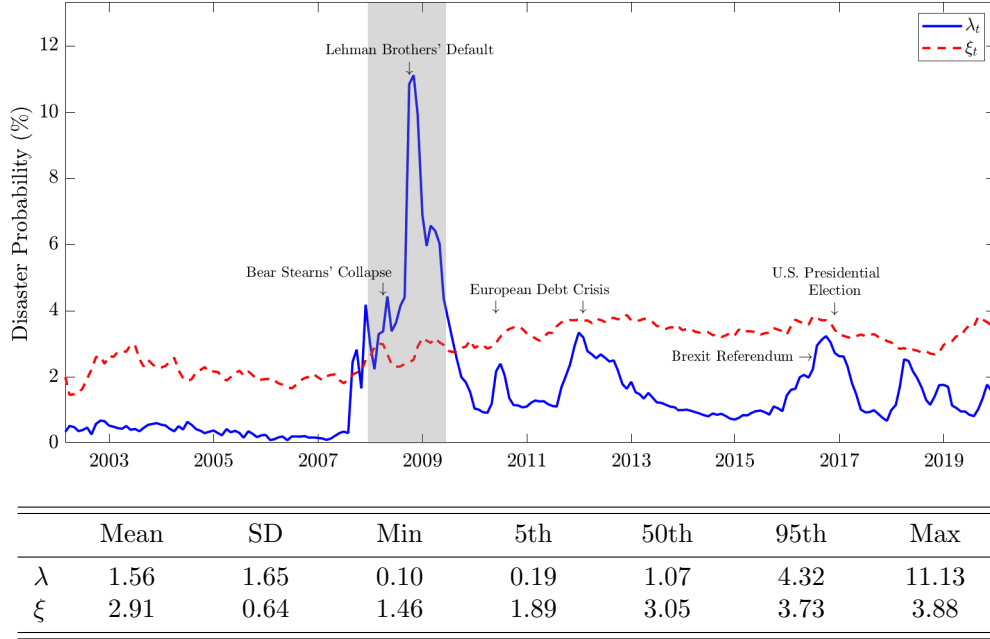


**Figure 4: Implied time-varying disaster risk.** This figure displays the filtered time series of the short-run disaster risk component  $\lambda_t$  (solid blue line) and the long-run disaster risk component  $\xi_t$  (dashed red line) from February 2002 to December 2019. Reported together are the mean, standard deviation, minimum, 5th percentile, median, 95th percentile, and maximum values for each time series. All values are expressed in percentage terms.

sample period.

While  $\lambda_t$  captures a fast-moving component of disaster risk,  $\xi_t$  captures a slow-moving component. The filtered time series in Figure 4 reveal that  $\xi_t$  is considerably less volatile than  $\lambda_t$  (with a standard deviation of 0.64% versus 1.65%) and moves slowly without deviating too much from its mean value. Moreover, we observe that  $\xi_t$  is far more persistent than  $\lambda_t$ : once it is hit by a large positive shock, it takes a long time for it to mean-revert back to its previous level. For instance, the level of  $\xi_t$  remained elevated during the post-Great Recession period. This is in sharp contrast with the behavior of  $\lambda_t$ , whose level quickly dropped even before the crisis was over.

Which aspect of the data makes it possible for us to characterize the time variation in crisis, exceeding the long-run component  $\xi_t$ , and then abruptly declined in the following months.

$\lambda_t$  and  $\xi_t$ , as discussed above? To understand how time-varying disaster risk is identified through our model, we conduct a sensitivity analysis. Figure 5 shows how the 3-, 6-, 12-month LIBOR-OIS spreads (Panel A) and the Black-implied volatilities for caps (Panel B) and swaptions (Panel C) change when we vary  $\lambda_t$  or  $\xi_t$  from the 5th percentile to the 95th percentile of its filtered values. In each panel, the solid blue lines describe the sensitivity with respect to  $\lambda_t$  while fixing  $\xi_t$  at the median, whereas the dashed red lines describe the sensitivity with respect to  $\xi_t$  while fixing  $\lambda_t$  at the median. Expected inflation  $q_t$  and mean consumption growth  $\mu_t$  are set at their median values in both cases. Lastly, the black dot in the middle of each bar represents the model value when  $\lambda_t$  and  $\xi_t$  are both at their median values.

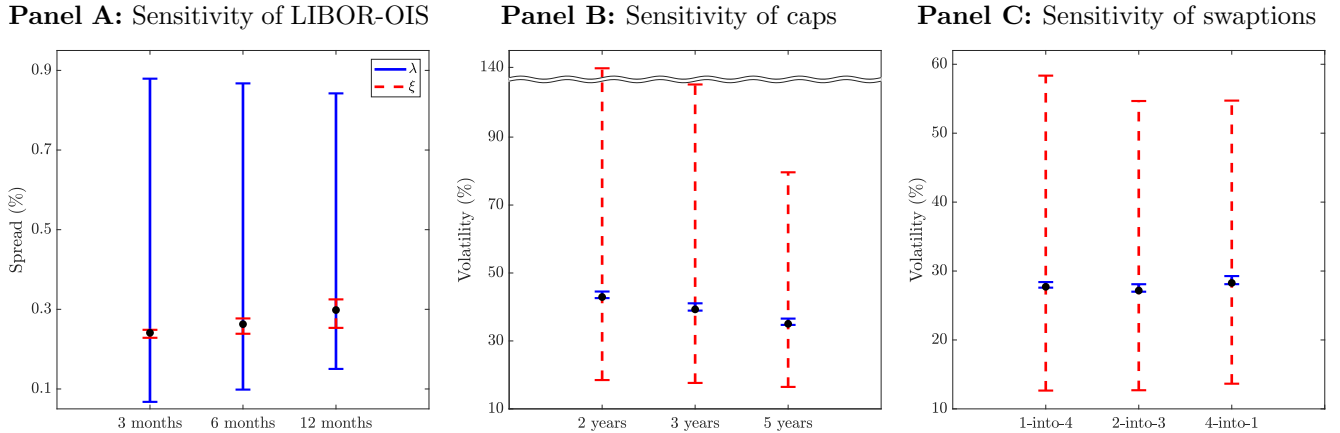


**Figure 5: Comparative statics.** This figure shows how the 3-, 6-, 12-month LIBOR-OIS spreads (Panel A) and the Black-implied volatilities for caps (Panel B) and swaptions (Panel C) change when  $\lambda_t$  or  $\xi_t$  varies from the 5th percentile to the 95th percentile of its filtered values. In each panel, the solid blue lines describe the sensitivity with respect to  $\lambda_t$  while fixing  $\xi_t$  at the median, whereas the dashed red lines describe the sensitivity with respect to  $\xi_t$  while fixing  $\lambda_t$  at the median. Expected inflation  $q_t$  and mean consumption growth  $\mu_t$  are set at their median values in both cases. The black dot in the middle of each bar represents the model value when  $\lambda_t$  and  $\xi_t$  are both at their median values. All values are expressed in percentage terms.

Panel A of Figure 5 reveals that the short-run component of disaster risk  $\lambda_t$  is mainly identified by the LIBOR-OIS spreads. While the LIBOR-OIS spreads increase with both  $\lambda_t$  and  $\xi_t$ , they are much more sensitive to  $\lambda_t$ . For example, the 3-month LIBOR-OIS spread

moves substantially, ranging from 0.1% to 0.9%, when  $\lambda_t$  varies between the 5th and 95th percentiles. In contrast, the 3-month LIBOR-OIS spread barely changes with respect to  $\xi_t$ , as can be seen in the panel.

These results are intuitive. The 3-month interbank rate is higher than the 3-month OIS rate because it is further influenced by the risk of a disaster happening over a 3-month horizon. Therefore, their gap, the 3-month LIBOR-OIS spread, is mostly sensitive to the short-run component of disaster risk. For the same reason,  $\xi_t$  plays a more noticeable role if a longer horizon is considered: from the panel, we find that the longest LIBOR-OIS spread with a 12-month maturity is more responsive to changes in  $\xi_t$ , compared to the 3-month LIBOR-OIS spread. However, the effect of  $\xi_t$  is still minuscule across all maturities, relative to the effect of  $\lambda_t$ . This confirms that the time series of the LIBOR-OIS spreads are the major channel through which the time variation of  $\lambda_t$  is identified.

Although the long-run component of disaster risk  $\xi_t$  has little impact on the LIBOR-OIS spreads, it has a large impact on interbank rate options. In Panels B and C of Figure 5, we discover completely opposite patterns. The Black-implied volatilities in both panels are highly sensitive to changes in  $\xi_t$ , whereas they are relatively less sensitive to changes in  $\lambda_t$ . The payoffs of caps and swaptions depend on future interbank rates over a long horizon ranging from 1 to 5 years. Hence, the pricing data on caps and swaptions play a critical role in characterizing the time variation of  $\xi_t$ .

Note that these model exercises are predicated on the assumption that both  $\lambda_t$  and  $\xi_t$  are time-varying. In the Internet Appendix, we estimate two nested cases of our model: (i) constant long-run mean of disaster risk (i.e., no variation in  $\xi_t$ ) and (ii) constant disaster risk (i.e., no variation in  $\lambda_t$ ). Based on the likelihood ratio test, the two nested models are

rejected, highlighting the significance of incorporating both time-varying  $\lambda_t$  and  $\xi_t$ .

In sum, our analysis demonstrates that both the short-run and long-run components of disaster risk are important model ingredients and are well identified using the data on interbank rates and their options.<sup>23</sup> It is worth emphasizing that the benefit of using interbank rate options is not limited to identifying the long-run component: the forward-looking information from caps and swaptions helps us accurately estimate the overall dynamics of disaster risk.

## 4.4 Implications for the equity market

Rare disaster models are often criticized as macro-finance models with “dark matter.” In order to explain the high equity premium and volatility in the postwar period, these models need to rely on the possibility of extremely bad events and its substantial time variation. However, it is not possible to measure disaster risk directly from the data, nor statistically test it with meaningful power, due to the rare nature of such events.

This dark matter criticism raises some concerns about how disaster risk models are calibrated: in typical variable disaster risk models, the dynamics of disaster risk are calibrated to match some key equity market moments, such as the equity premium and the market volatility. However, Chen, Dou, and Kogan (2024) point out that a model with economic dark matter is likely to be fragile due to the lack of internal refutability and poor out-of-sample performance. Addressing this criticism is challenging: as discussed by Cochrane (2017), it requires either independently anchoring time-varying disaster risk to some data or reconciling multiple asset classes under one consistent assumption about disaster risk.

---

<sup>23</sup>In addition, the Internet Appendix provides a discussion of how the short-run and long-run components of disaster risk differently affect the instantaneous bond variance.

Our analysis highlights that the interbank market can potentially be useful for addressing the dark matter criticism. We make a plausible assumption that consumption disasters are likely to coincide with interbank market failure. This identification assumption makes it possible to extract time-varying disaster risk that is manifested in LIBOR-OIS spreads as well as caps and swaptions. Since our estimation does not depend on equity market moments, our results can serve as an external/out-of-sample validity test of disaster risk models for the equity market. The parameter estimates from Section 4.1 suggest that the estimated disaster dynamics are fairly close to those implied by Seo and Wachter (2018), whose calibration is primarily based on the equity market. Overall, our finding that disaster risk is significant in size and in variation strongly supports a disaster-based explanation of various asset pricing puzzles (Gabaix, 2012; Wachter, 2013).

An additional advantage of our approach is that we obtain the past time series of the short-run and long-run components of disaster risk, namely  $\lambda_t$  and  $\xi_t$ . These time series provide an extra basis for testing the implications of disaster risk for the equity market. First of all, Panel A of Table 4 considers the following conditional moments that are associated with the equity market: the price-dividend ratio ( $\log P/D$ ), price-earnings ratio ( $\log P/E$ ), implied variance (IV), expected realized variance (ERV), and variance risk premium (VRP).<sup>24</sup> Since these conditional moments are functions of disaster risk in variable disaster risk models, one testable implication is that their time series variations should be explained by disaster-related state variables.

Hence, we run contemporaneous linear regressions of the five conditional equity market moments at time  $t$  on  $\lambda_t$  and  $\xi_t$ . We standardize both independent and dependent variables

---

<sup>24</sup>The price-dividend and price-earnings ratios are downloaded from Robert Shiller's website. The three variance-related variables are downloaded from Hao Zhou's website.



<b>Panel A: Valuation ratios and variance-related variables</b>						
		(1) log P/D	(2) log P/E	(3) IV	(4) ERV	(5) VRP
$\lambda_t$	Coef.	-0.68	-0.53	0.72	0.64	0.37
	<i>t</i> -stat	[-5.13]	[-4.18]	[5.54]	[3.54]	[2.81]
$\xi_t$	Coef.	-0.48	-0.20	0.02	0.06	-0.05
	<i>t</i> -stat	[-7.25]	[-2.63]	[0.31]	[1.01]	[-0.80]
Adj $R^2$ (%)		68.69	31.87	52.30	41.29	13.83
<b>Panel B: Out-of-the-money put option prices</b>						
		(1) 1 month	(2) 3 months	(3) 6 months	(4) 9 months	(5) 12 months
$\lambda_t$	Coef.	0.70	0.68	0.65	0.58	0.39
	<i>t</i> -stat	[5.38]	[5.78]	[5.34]	[5.18]	[4.62]
$\xi_t$	Coef.	0.04	0.11	0.21	0.31	0.31
	<i>t</i> -stat	[0.62]	[1.46]	[2.67]	[3.88]	[4.02]
Adj $R^2$ (%)		49.28	47.21	46.52	43.05	24.49

**Table 4: Disaster risk and conditional equity moments.** This table reports the results of contemporaneous time series regressions that examine the relation between the filtered disaster risk variables ( $\lambda_t$  and  $\xi_t$ ) and conditional equity market moments. Since  $\lambda_t$  and  $\xi_t$  are correlated, we take the orthogonal component of  $\lambda_t$  with respect to  $\xi_t$ . In both panels, we standardize the independent and dependent variables. In Panel A, the dependent variables are the log price-dividend ratio (log P/D), log price-earnings ratio (log P/E), implied variance (IV), expected realized variance (ERV), and the variance risk premium (VRP). In Panel B, the dependent variables are the prices of S&P 500 put options with 90% moneyness, normalized by the underlying index level. We consider options with maturities of 1, 3, 6, 9, and 12 months. The *t*-statistics, shown in brackets, are computed using the Newey and West (1987) method with four lags.

in our regressions to facilitate the interpretation of slope coefficients. In columns (1) and (2) of Panel A, we document that the valuation ratios fall when  $\lambda_t$  and  $\xi_t$  rise. For instance, a one standard deviation increase in  $\lambda_t$  leads to a 0.68 standard deviation drop in the log price-dividend ratio. A one standard deviation increase in  $\xi_t$  leads to a 0.48 standard deviation drop in the log price-dividend ratio. These negative relations are statistically significant with high *t*-statistics. These results are consistent with economic intuition as well as empirical evidence: stock market valuations are low in bad economic times with high disaster risk.

In columns (3), (4), and (5), we examine the relation between disaster risk and each of the three variance-related variables. Note that the implied variance and the expected realized variance measure the risk-neutral and physical expectations of future 1-month equity market

variance, respectively. The variance risk premium, calculated as their difference, captures compensation for taking variance risk over a 1-month horizon. We expect positive relations from our regression because higher disaster risk results in higher variance risk as well as higher compensation for variance risk. In line with this, we find a strong positive relation between the short-run component of disaster risk  $\lambda_t$  and each variance-related variable. However, we find that the impact of the long-run component  $\xi_t$  is insignificant. This is not surprising, since the variance-related variables are based on a very short horizon, namely, a month.

Panel B of Table 4 considers out-of-the-money put option prices as additional conditional moments since they are particularly informative about tail events. At each point in time, we obtain the prices of S&P 500 put options with 90% moneyness, normalized by the underlying index price.<sup>25</sup> This normalization allows us to compare option prices at different points in time by removing the effect of the index level. Columns (1)–(5) report the results from contemporaneous linear regressions of the normalized prices of put options with 1-, 3-, 6-, 9-, and 12-month maturities on the time series of  $\lambda_t$  and  $\xi_t$ . Column (1) of Panel B demonstrates that  $\lambda_t$  significantly and positively explains the 1-month put option price while  $\xi_t$  has no statistically significant impact. This is consistent with the results for the 1-month-ahead implied variance in Panel A. Comparing the five columns in Panel B, we can see that  $\lambda_t$  is significant across all maturities. In the case of  $\xi_t$ , its economic magnitude and statistical significance gradually increase as option maturity increases. As a result, the effect of  $\xi_t$  becomes significant for maturities longer than or equal to 6 months. These results are sensible:

---

<sup>25</sup>We download options data from OptionMetrics. Since we do not observe options with fixed moneyness or a constant maturity every day, we use a regression-based interpolation of implied volatilities with respect to moneyness and maturity by adopting the methodology of Seo and Wachter (2019). The price of an option with a specific moneyness and a specific maturity is, then, calculated by plugging the interpolated implied volatility into the Black-Scholes formula.

the long-run component of disaster risk  $\xi_t$  better explains long-horizon equity moments, such as the price-dividend ratio, price-earnings ratio, and longer-term option prices.

<b>Panel A: Factor portfolios</b>						
		(1) MktRf	(2) SMB	(3) HML	(4) MOM	(5) LIQ
$\Delta\lambda_t$	Coef.	-0.22	-0.09	0.12	0.09	-0.14
	<i>t</i> -stat	[-4.98]	[-2.20]	[1.36]	[1.12]	[-1.27]
$\Delta\xi_t$	Coef.	-0.35	-0.27	-0.15	0.17	-0.30
	<i>t</i> -stat	[-5.33]	[-4.95]	[-1.80]	[2.04]	[-3.10]
Adj $R^2$ (%)		14.64	6.92	3.50	2.91	9.62
<b>Panel B: Fama-French 10 industry portfolios</b>						
		(1) Durbl	(2) Manuf	(3) HiTec	(4) Telcm	(5) Shops
$\Delta\lambda_t$	Coef.	-0.15	-0.23	-0.21	-0.23	-0.16
	<i>t</i> -stat	[-4.62]	[-4.12]	[-5.89]	[-6.00]	[-4.99]
$\Delta\xi_t$	Coef.	-0.34	-0.33	-0.38	-0.28	-0.27
	<i>t</i> -stat	[-7.10]	[-6.09]	[-4.92]	[-3.75]	[-3.96]
Adj $R^2$ (%)		12.41	14.19	16.31	11.00	8.74
		(6) Enrgy	(7) Hlth	(8) NoDur	(9) Utils	(10) Other
$\Delta\lambda_t$	Coef.	-0.19	-0.18	-0.13	-0.25	-0.16
	<i>t</i> -stat	[-3.96]	[-3.06]	[-2.15]	[-3.92]	[-3.21]
$\Delta\xi_t$	Coef.	-0.29	-0.19	-0.15	-0.09	-0.33
	<i>t</i> -stat	[-5.13]	[-2.95]	[-2.05]	[-0.78]	[-5.10]
Adj $R^2$ (%)		9.99	5.65	3.14	5.91	11.67

**Table 5: Shocks to disaster risk and equity returns.** This table reports the results of contemporaneous time series regressions that examine the relation between changes in the filtered disaster risk variables ( $\lambda_t$  and  $\xi_t$ ) and equity returns. In both panels, we standardize the independent and dependent variables. In Panel A, the dependent variables are the excess market return (MktRf), size factor return (SMB), book-to-market factor return (HML), momentum factor return (MOM), and liquidity factor return (LIQ). In Panel B, the dependent variables are the excess returns on the 10 Fama-French industry portfolios. These industries include consumer durables (Durbl), manufacturing (Manuf), business equipment (HiTec), telecommunication (Telcm), retail (Shops), energy (Enrgy), healthcare (Hlth), consumer non-durables (NoDur), utilities (Utils), and others (Other). The *t*-statistics, shown in brackets, are computed using the Newey and West (1987) method with four lags.

So far, we have examined whether disaster risk can explain the variations in conditional equity market moments. Another testable implication of disaster risk for the equity market is that equity returns should be negatively associated with shocks to  $\lambda_t$  and  $\xi_t$ . Panel A of Table 5 reports the results from regressing the market, size, value, momentum, and liquidity

factors on changes in  $\lambda_t$  and  $\xi_t$ .<sup>26</sup> We find that changes in both the short-run and long-run components of disaster risk are indeed negatively related to the market, size, and liquidity factors. This implies that  $\lambda_t$  and  $\xi_t$  capture more than just aggregate market risk.

Lastly, Panel B of Table 5 investigates how shocks to disaster risk affect contemporaneous excess returns on the Fama-French 10 industry portfolios. Intuitively, some industries are less sensitive to disaster risk than others. For example, industries that focus on consumer staples, such as food and utilities, are likely to be less exposed to disaster risk. This intuition is confirmed in Panel B: the relations between changes in disaster risk and industry returns show relatively smaller t-statistics for industries including consumer non-durables and utilities (columns (8)-(9)). In contrast, for industries that are more business-cycle sensitive, such as consumer durables, manufacturing, business equipment, telecommunication, and retail (columns (1)-(5)), we obtain more significant negative relations.

## 5 Conclusion

While prior studies on rare disasters calibrate time-varying disaster risk, accurately characterizing it from the data remains a considerable challenge. This is extremely difficult because disasters are nearly unobservable events in the post-war sample. In order to tackle this issue, our paper ties time-varying probabilities of disasters to an independent source of data: interbank rates and their options.

Our approach relies on the assumption that macroeconomic disasters are likely to coincide with interbank market failure. This link allows us to derive the model-implied interest

---

<sup>26</sup>The market, size, and value factors follow Fama and French (1993), and the momentum factor follows Fama and French (2012). These time series are downloaded from Kenneth French's website. The liquidity risk factor follows Pastor and Stambaugh (2003) and is downloaded from Robert Stambaugh's website.

rate spreads and option prices on interbank rates as functions of the short-run and long-run components of disaster risk. We show that these data are particularly sensitive to disaster risk, which enables us to reliably infer not only the level of disaster probabilities but also their dynamics.

The estimation results suggest that disaster risk is significant in size and in variation, strongly upholding the validity of macro-finance models with the rare disaster mechanism. Using the filtered time series of the short-run and long-run components of disaster risk, we confirm that the implications of these models for equity moments and equity returns are consistent with empirical evidence. Overall, our analysis highlights that interest rates and their options can be valuable tools for deepening our understanding of extreme economic tail risk.

# Appendix

## A Model derivations

### A.1 Risk-neutral dynamics

Given the assumption about the pricing kernel in equation (4), the Brownian shocks under the risk-neutral measure are written as follows:

$$\begin{aligned}dB_{C,t}^Q &= dB_{C,t} + \theta_C dt, \\dB_{\mu,t}^Q &= dB_{\mu,t} + \theta_\mu dt, \\dB_{\lambda,t}^Q &= dB_{\lambda,t} + \theta_\lambda \sqrt{\lambda_t} dt, \\dB_{\xi,t}^Q &= dB_{\xi,t} + \theta_\xi \sqrt{\xi_t} dt, \\dB_{q,t}^Q &= dB_{q,t} + \theta_q dt.\end{aligned}$$

Moreover, under the risk-neutral measure, the disaster intensity and the moment generating function (MGF) of the jump size distributions are represented as

$$\begin{aligned}\lambda_t^Q &= \lambda_t \Phi_Z(\theta_N, 0, 0), \\ \mathbb{E}^Q \left[ e^{u_1 Z_C + u_2 Z_L + u_3 Z_q} \right] &= \frac{\Phi_Z(u_1 + \theta_N, u_2, u_3)}{\Phi_Z(\theta_N, 0, 0)},\end{aligned}$$

where  $\Phi_Z(u_1, u_2, u_3) = \mathbb{E} [e^{u_1 Z_C + u_2 Z_L + u_3 Z_q}]$  is the MGF of  $(Z_C, Z_L, Z_q)$  under the physical measure. This leads to the following risk-neutral dynamics of the underlying processes,

$$\begin{aligned}\frac{dC_t}{C_t} &= \mu_C^Q dt + \sigma_C dB_{C,t}^Q + (e^{Z_{C,t}} - 1) dN_t, \\ d\mu_t &= \kappa_\mu^Q (\bar{\mu}^Q - q_t) dt + \sigma_\mu dB_{\mu,t}^Q \\ d\lambda_t &= \kappa_\lambda^Q (\nu \xi_t - \lambda_t) dt + \sigma_\lambda \sqrt{\lambda_t} dB_{\lambda,t}^Q, \\ d\xi_t &= \kappa_\xi^Q (\bar{\xi}^Q - \xi_t) dt + \sigma_\xi \sqrt{\xi_t} dB_{\xi,t}^Q, \\ dq_t &= \kappa_q^Q (\bar{q}^Q - q_t) dt + \sigma_q dB_{q,t}^Q + Z_{q,t} dN_t,\end{aligned}$$

where  $\mu_C^Q = \mu_C - \theta_C \sigma_C$ ,  $\kappa_\mu^Q = \kappa_\mu$ ,  $\bar{\mu}^Q = \frac{\kappa_\mu \bar{\mu} - \theta_\mu \sigma_\mu}{\kappa_\mu^Q}$ ,  $\kappa_\lambda^Q = \kappa_\lambda + \sigma_\lambda \theta_\lambda$ ,  $\nu = \frac{\kappa_\lambda}{\kappa_\lambda^Q}$ ,  $\kappa_\xi^Q = \kappa_\xi + \sigma_\xi \theta_\xi$ ,  $\bar{\xi}^Q = \frac{\kappa_\xi \bar{\xi}}{\kappa_\xi^Q}$ ,  $\kappa_q^Q = \kappa_q$ , and  $\bar{q}^Q = \frac{\kappa_q \bar{q} - \theta_q \sigma_q}{\kappa_q^Q}$ .

## A.2 Zero-coupon yields

The time- $t$  value of \$1 zero-coupon interbank lending maturing at time  $t + \tau$  is written as

$$P_i(t, t + \tau) = \mathbb{E}_t^Q \left[ e^{-\int_t^{t+\tau} r_u du} \frac{L_{t+\tau}}{L_t} \right].$$

By multiplying both sides of the above equation with  $e^{-\int_0^t r_u du} L_t$ , we obtain the following martingale:

$$e^{-\int_0^t r_u du} P_i(t, t + \tau) L_t = \mathbb{E}_t^Q \left[ e^{-\int_0^{t+\tau} r_u du} L_{t+\tau} \right].$$

We conjecture that the price of a zero-coupon interbank lending is expressed as

$$P_i(t, t + \tau) = \exp(a_i(\tau) + b_{i,\lambda}(\tau) \lambda_t + b_{i,\xi}(\tau) \xi_t + b_{i,\mu}(\tau) \mu_t + b_{i,q}(\tau) q_t),$$

and its stochastic differential equation is given as

$$\begin{aligned}
\frac{dP_{i,t}}{P_{i,t^-}} = & \left( b_{i,\lambda}(\tau)\kappa_\lambda^Q(\nu\xi_t - \lambda_t) + b_{i,\xi}(\tau)\kappa_\xi^Q(\bar{\xi}^Q - \xi_t) + b_{i,\mu}(\tau)\kappa_\mu^Q(\bar{\mu}^Q - \mu_t) + b_{i,q}(\tau)\kappa_q^Q(\bar{q}^Q - q_t) \right. \\
& + \frac{1}{2}b_{i,\lambda}(\tau)^2\sigma_\lambda^2\lambda_t + \frac{1}{2}b_{i,\xi}(\tau)^2\sigma_\xi^2\xi_t + \frac{1}{2}b_{i,\mu}(\tau)^2\sigma_\mu^2 + \frac{1}{2}b_{i,q}(\tau)^2\sigma_q^2 \\
& \left. - (a'_i(\tau) + b'_{i,\lambda}(\tau)\lambda_t + b'_{i,\xi}(\tau)\xi_t + b'_{i,\mu}(\tau)\mu_t + b'_{i,q}(\tau)q_t) \right) dt \\
& + b_{i,\lambda}(\tau)\sigma_\lambda\sqrt{\lambda_t}dB_{\lambda,t}^Q + b_{i,\xi}(\tau)\sigma_\xi\sqrt{\xi_t}dB_{\xi,t}^Q + b_{i,\mu}(\tau)\sigma_\mu dB_{\mu,t}^Q + b_{i,q}(\tau)\sigma_q dB_{q,t}^Q \\
& + (e^{b_{i,q}(\tau)Z_{q,t}} - 1) dN_t.
\end{aligned}$$

Since  $(e^{-\int_0^t r_u du} P_{i,t}(\tau) L_t)$  is a martingale, the sum of the drift and the jump compensator should be zero. This martingale property provides the system of ordinary differential equations (ODEs) for  $a_i$ ,  $b_{i,\lambda}$ ,  $b_{i,\xi}$ ,  $b_{i,\mu}$ , and  $b_{i,q}$  as follows:

$$\begin{aligned}
a'_i(\tau) &= -\delta_0 + b_{i,\xi}(\tau)\kappa_\xi^Q\bar{\xi}^Q + b_{i,\mu}(\tau)\kappa_\mu^Q\bar{\mu}^Q + b_{i,q}(\tau)\kappa_q^Q\bar{q}^Q + \frac{1}{2}b_{i,\mu}(\tau)^2\sigma_\mu^2 + \frac{1}{2}b_{i,q}(\tau)^2\sigma_q^2, \\
b'_{i,\lambda}(\tau) &= -\delta_\lambda - b_{i,\lambda}(\tau)\kappa_\lambda^Q + \frac{1}{2}b_{i,\lambda}(\tau)^2\sigma_\lambda^2 \\
&\quad + \bar{p}\Phi_Z(\theta_N, 1, b_{i,q}(\tau)) + (1 - \bar{p})\Phi_Z(\theta_N, 0, b_{i,q}(\tau)) - \Phi_Z(\theta_N, 0, 0), \\
b'_{i,\xi}(\tau) &= -\delta_\xi + b_{i,\lambda}(\tau)\kappa_\lambda^Q\nu - b_{i,\xi}(\tau)\kappa_\xi^Q + \frac{1}{2}b_{i,\xi}(\tau)^2\sigma_\xi^2, \\
b'_{i,\mu}(\tau) &= -\delta_\mu - b_{i,\mu}(\tau)\kappa_\mu^Q, \\
b'_{i,q}(\tau) &= -\delta_q - b_{i,q}(\tau)\kappa_q^Q,
\end{aligned}$$

with the initial condition:  $a_i(0) = b_{i,\lambda}(0) = b_{i,\xi}(0) = b_{i,\mu}(0) = b_{i,q}(0) = 0$ .



Similarly, the price of \$1 zero-coupon risk-free lending is given by

$$P_f(t, t + \tau) = \mathbb{E}_t^Q \left[ e^{-\int_t^{t+\tau} r_u du} \cdot 1 \right],$$

and we conjecture the price has the form of

$$P_f(t, t + \tau) = \exp(a_f(\tau) + b_{f,\lambda}(\tau)\lambda_t + b_{f,\xi}(\tau)\xi_t + b_{f,\mu}(\tau)\mu_t + b_{f,q}(\tau)q_t).$$

Since  $\left( e^{-\int_0^t r_u du} P_{f,t}(\tau) \right)$  is a martingale, the sum of the drift and the jump compensator should be zero. This martingale property provides the following system of ODEs for  $a_f$ ,  $b_{f,\lambda}$ ,  $b_{f,\xi}$ ,  $b_{f,\mu}$ , and  $b_{f,q}$ :

$$\begin{aligned} a'_f(\tau) &= -\delta_0 + b_{f,\xi}(\tau)\kappa_\xi^Q \bar{\xi}^Q + b_{f,\mu}(\tau)\kappa_\mu^Q \bar{\mu}^Q + b_{f,q}(\tau)\kappa_q^Q \bar{q}^Q + \frac{1}{2}b_{f,\mu}(\tau)^2\sigma_\mu^2 + \frac{1}{2}b_{f,q}(\tau)^2\sigma_q^2, \\ b'_{f,\lambda}(\tau) &= -\delta_\lambda - b_{f,\lambda}(\tau)\kappa_\lambda^Q + \frac{1}{2}b_{f,\lambda}(\tau)^2\sigma_\lambda^2 + \Phi_Z(\theta_N, 0, b_{f,q}(\tau)) - \Phi_Z(\theta_N, 0, 0), \\ b'_{f,\xi}(\tau) &= -\delta_\xi + b_{f,\lambda}(\tau)\kappa_\lambda^Q \nu - b_{f,\xi}(\tau)\kappa_\xi^Q + \frac{1}{2}b_{f,\xi}(\tau)^2\sigma_\xi^2, \\ b'_{f,\mu}(\tau) &= -\delta_\mu - b_{f,\mu}(\tau)\kappa_\mu^Q, \\ b'_{f,q}(\tau) &= -\delta_q - b_{f,q}(\tau)\kappa_q^Q, \end{aligned}$$

with the initial conditions:  $a_f(0) = b_{f,\lambda}(0) = b_{f,\xi}(0) = b_{f,\mu}(0) = b_{f,q}(0) = 0$ . Note that  $b_{i,\mu}(\tau)$  and  $b_{f,\mu}(\tau)$  are identical, and so are  $b_{i,q}(\tau)$  and  $b_{f,q}(\tau)$ , as their ODEs are identical with the same initial conditions. Therefore, we simply denote them as  $b_\mu(\tau)$  and  $b_q(\tau)$ , respectively.

Now we turn to the Treasury rate. The stochastic differential equation for  $x_t$  implies that

for any  $u \geq t$ ,

$$x_u = x_t e^{-\kappa_x(u-t)} + \bar{x} (1 - e^{-\kappa_x(u-t)}) + \int_0^{u-t} \sigma_x e^{-\kappa_x(u-t-s)} dB_{x,s}.$$

Clearly,  $x_u$  is Gaussian and so is  $\left(\int_t^{t+\tau} x_u du\right)$ . Hence, the expression for  $\mathbb{E}_t \left[ e^{\int_t^{t+\tau} x_u du} \right]$  in equation (8) can be derived using the moment generating function of a normal distribution.

This leads us to the following deterministic functions  $a_x$  and  $b_x$  shown in equation (8):

$$\begin{aligned} a_x(\tau) &= \left( \bar{x} + \frac{\sigma_x^2}{2\kappa_x^2} \right) \left[ \frac{1 - e^{-\kappa_x \tau}}{\kappa_x} - \tau \right] + \frac{\sigma_x^2}{4\kappa_x} \left[ \frac{1 - e^{-\kappa_x \tau}}{\kappa_x} \right]^2, \\ b_x(\tau) &= - \left( \frac{1 - e^{-\kappa_x \tau}}{\kappa_x} \right). \end{aligned}$$

Based on the identity  $y_{g,t}^{(\tau)} = y_{f,t}^{(\tau)} - y_{x,t}^{(\tau)}$ , the  $\tau$ -maturity Treasury rate  $y_{g,t}^{(\tau)}$  is obtained by

$$y_{g,t}^{(\tau)} = -\frac{1}{\tau} \left[ a_f(\tau) - a_x(\tau) + b_{f,\lambda}(\tau)\lambda_t + b_{f,\xi}(\tau)\xi_t + b_\mu(\tau)\mu_t + b_q(\tau)q_t - b_x(\tau)x_t \right].$$

### A.3 Cap and swaption pricing

Before deriving the expressions for the prices of caps and swaptions, we first find the pricing formula for a put option on  $P_i(T_0, T_1)$  with a strike price  $K$ . Following Duffie, Pan, and Singleton (2000), Collin-Dufresne and Goldstein (2003), and Trolle and Schwartz (2009), we compute the put option price by using the transform analysis:

$$\begin{aligned} \mathcal{P}(t, T_0, T_1, K) &= \mathbb{E}_t^Q \left[ e^{-\int_t^{T_0} r_s ds} (K - P_i(T_0, T_1)) \mathbb{1}_{\{P_i(T_0, T_1) < K\}} \right] \\ &= KG_{0,1}(\log K) - G_{1,1}(\log K), \end{aligned}$$

where

$$G_{a,b}(y) = \frac{\psi(a, t, T_0, T_1)}{2} - \frac{1}{\pi} \int_0^\infty \frac{\text{Im} [\psi(a + iub, t, T_0, T_1) e^{-iuy}]}{u} du,$$

$$\psi(u, t, T_0, T_1) = \mathbb{E}_t^Q \left[ \exp \left( - \int_t^{T_0} r_s ds \right) e^{u \log(P_i(T_0, T_1))} \right].$$

Note that the function  $\psi$  solves the complex-valued ODEs of Duffie, Pan, and Singleton (2000), and the operator  $\text{Im}[\cdot]$  represents the imaginary part of a complex number.

The time- $t$  cap price is given by equation (9). Under the approximation  $e^{-\int_{t_j}^{t_{j+1}} r_s ds} \approx P_i(t_j, t_{j+1})$ , we re-express the cap pricing formula as

$$V_{\text{cap}}^{(T)}(t, K) \approx \sum_{j=1}^{m_T} \mathbb{E}_t^Q \left[ \exp \left( - \int_t^{t_j} r_s ds \right) P_i(t_j, t_{j+1}) \left[ \frac{1}{P_i(t_j, t_{j+1})} - 1 - \Delta \times K \right]^+ \right]$$

$$= (1 + \Delta \times K) \sum_{j=1}^{m_T} \mathcal{P} \left( t, t_j, t_{j+1}, \frac{1}{1 + \Delta \times K} \right).$$

As discussed in Section 2.4, we price swaptions by adopting the stochastic duration method suggested by Wei (1997), Munk (1999), and Trolle and Schwartz (2009). Applying this method to equation (10) results in:

$$V_{\text{payer}}^{(T, \bar{T})}(t, K) = \mathbb{E}_t^Q \left[ \exp \left( - \int_t^{t+T} r_s ds \right) \left[ 1 - V_{\text{fixed}}^{(\bar{T})}(t + T, K) \right]^+ \right]$$

$$\approx \zeta \mathcal{P}(t, T, t + \mathcal{D}(t, T, \bar{T}), \zeta^{-1}),$$

where  $\zeta = \frac{\sum_{l=1}^{\bar{T}/\Delta} Y_l P_i(t, t+T+l\Delta)}{P_i(t, t+\mathcal{D}(t, T, \bar{T}))}$ . The stochastic duration  $\mathcal{D}(t, T, \bar{T})$ , or simply  $\mathcal{D}(t)$ , is defined

as a quantity that satisfies:

$$\begin{aligned}
& b_{i,\lambda}(\mathcal{D}(t))^2 \sigma_\lambda^2 \lambda_t + b_{i,\xi}(\mathcal{D}(t))^2 \sigma_\xi^2 \xi_t + b_q(\mathcal{D}(t))^2 \sigma_q^2 + b_\mu(\mathcal{D}(t))^2 \sigma_\mu^2 \\
& + [\Phi(\theta_N, 0, 2b_q(\mathcal{D}(t))) - 2\Phi(\theta_N, 0, b_q(\mathcal{D}(t))) + \Phi(\theta_N, 0, 0)] \lambda_t \\
& = \left[ \sum_{j=1}^{\bar{T}/\Delta} w_j b_{i,\lambda}(T + j\Delta) \right]^2 \sigma_\lambda^2 \lambda_t + \left[ \sum_{j=1}^{\bar{T}/\Delta} w_j b_{i,\xi}(T + j\Delta) \right]^2 \sigma_\xi^2 \xi_t + \left[ \sum_{j=1}^{\bar{T}/\Delta} w_j b_q(T + j\Delta) \right]^2 \sigma_q^2 \\
& + \left[ \sum_{j=1}^{\bar{T}/\Delta} w_j b_\mu(T + j\Delta) \right]^2 \sigma_\mu^2 + \left[ \sum_{j=1}^{\bar{T}/\Delta} \left[ w_j^2 \Phi(\theta_N, 0, 2b_q(T + j\Delta)) - 2w_j \Phi(\theta_N, 0, b_q(T + j\Delta)) \right. \right. \\
& \quad \left. \left. + \sum_{k>j} 2w_j w_k \Phi(\theta_N, 0, b_q(T + j\Delta) + b_q(T + k\Delta)) \right] + \Phi(\theta_N, 0, 0) \right] \lambda_t,
\end{aligned}$$

where  $w_j = \frac{Y_j P_i(t, t+T+j\Delta)}{\sum_{l=1}^{\bar{T}/\Delta} Y_l P_i(t, t+T+l\Delta)}$ ,  $Y_j = \Delta \times K$  for  $j = 1, 2, \dots, \frac{\bar{T}}{\Delta} - 1$ , and  $Y_{\bar{T}/\Delta} = 1 + \Delta \times K$ .

## References

- Acharya, Viral V., and David Skeie, 2011, A model of liquidity hoarding and term premia in inter-bank markets, *Journal of Monetary Economics* 58, 436–447.
- Adrian, Tobias, Erko Etula, and Tyler Muir, 2014, Financial intermediaries and the cross-section of asset returns, *Journal of Finance* 69, 2557–2596.
- Allen, Linda, Turan G. Bali, and Yi Tang, 2012, Does systemic risk in the financial sector predict future economic downturns?, *Review of Financial Studies* 25, 3000–3036.
- Andersen, Torben G., Nicola Fusari, and Viktor Todorov, 2015, The risk premia embedded in index options, *Journal of Financial Economics* 117, 558–584.
- Ang, Andrew, and Monika Piazzesi, 2003, A no-arbitrage vector autoregression of term structure dynamics with macroeconomic and latent variables, *Journal of Monetary Economics* 50, 745–787.
- Bakshi, Gurdip, John Crosby, Xiaohui Gao, and Jorge W. Hansen, 2023, Treasury option returns and models with unspanned risks, *Journal of Financial Economics* 150, 103736.
- Bakshi, Gurdip, Xiaohui Gao, and Jinming Xue, 2023, Recovery with applications to forecasting equity disaster probability and testing the spanning hypothesis in the treasury market, *Journal of Financial and Quantitative Analysis* pp. 1–35.
- Barro, Robert J., 2006, Rare disasters and asset markets in the twentieth century, *Quarterly Journal of Economics* 121, 823–866.

- Barro, Robert J., and José F. Ursúa, 2008, Macroeconomic crises since 1870, *Brookings Papers on Economic Activity* no. 1, 255–350.
- Berkman, Henk, Ben Jacobsen, and John B. Lee, 2011, Time-varying rare disaster risk and stock returns, *Journal of Financial Economics* 101, 313–332.
- Bernanke, Ben S., 1983, Nonmonetary effects of the financial crisis in the propagation of the Great Depression, *American Economic Review* 73, 257–276.
- Black, Fischer, 1976, The pricing of commodity contracts, *Journal of Financial Economics* 3, 167–179.
- Bollerslev, Tim, and Viktor Todorov, 2011a, Estimation of jump tails, *Econometrica* 79, 1727–1783.
- Bollerslev, Tim, and Viktor Todorov, 2011b, Tails, fears, and risk premia, *Journal of Finance* 66, 2165–2211.
- Bollerslev, Tim, and Viktor Todorov, 2014, Time-varying jump tails, *Journal of Econometrics* 183, 168–180.
- Brunnermeier, Markus K., and Yuliy Sannikov, 2014, A macroeconomic model with a financial sector, *American Economic Review* 104, 379–421.
- Chen, Hui, Winston Wei Dou, and Leonid Kogan, 2024, Measuring “dark matter” in asset pricing models, *Journal of Finance* 79, 843–902.
- Chen, Ren-raw, and Louis Scott, 2003, Multi-factor Cox-Ingersoll-Ross models of the term structure: Estimates and tests from a Kalman filter model, *Journal of Real Estate Finance and Economics* 27, 143–172.
- Christoffersen, Peter, Christian Dorion, Kris Jacobs, and Lotfi Karoui, 2014, Nonlinear Kalman filtering in affine term structure models, *Management Science* 60, 2248–2268.
- Cochrane, John H., 2017, Macro-finance, *Review of Finance* 21, 945–985.
- Collin-Dufresne, Pierre, and Robert Goldstein, 2003, Generalizing the affine framework to HJM and random field models, *Working paper*.
- Doshi, Hitesh, Redouane Elkamhi, and Chayawat Ornthanalai, 2018, The term structure of expected recovery rates, *Journal of Financial and Quantitative Analysis* 53, 2619–2661.
- Duan, Jin-Chuan, and Jean-Guy Simonato, 1999, Estimating and testing exponential-affine term structure models by Kalman filter, *Review of Quantitative Finance and Accounting* 13, 111–135.
- Duffee, Gregory R, 1999, Estimating the price of default risk, *Review of Financial Studies* 12, 197–226.
- Duffie, Darrell, 2005, Credit risk modeling with affine processes, *Journal of Banking & Finance* 29, 2751–2802.
- Duffie, Darrell, Jun Pan, and Kenneth Singleton, 2000, Transform analysis and asset pricing for affine jump-diffusions, *Econometrica* 68, 1343–1376.
- Duffie, Darrell, and Kenneth J Singleton, 1999, Modeling term structures of defaultable bonds, *Review of Financial Studies* 12, 687–720.
- Fama, Eugene F., and Kenneth R. French, 1993, Common risk factors in the returns on bonds and stocks, *Journal of Financial Economics* 33, 3–56.
- Fama, Eugene F., and Kenneth R. French, 2012, Size, value, and momentum in international stock returns, *Journal of Financial Economics* 105, 457–472.
- Filipović, Damir, and Anders B. Trolle, 2013, The term structure of interbank risk, *Journal of Financial Economics* 109, 707–733.

- Gabaix, Xavier, 2012, An exactly solved framework for ten puzzles in macro-finance, *Quarterly Journal of Economics* 127, 645–700.
- Giesecke, Kay, Francis A. Longstaff, Stephen Schaefer, and Ilya A. Strebulaev, 2014, Macroeconomic effects of corporate default crisis: A long-term perspective, *Journal of Financial Economics* 111, 297–310.
- Gourio, François, 2012, Disaster risk and business cycles, *American Economic Review* 102, 2734–2766.
- Han, Bing, 2007, Stochastic volatilities and correlations of bond yields, *Journal of Finance* 62, 1491–1524.
- Haubrich, Joseph, George Pennacchi, and Peter Ritchken, 2012, Inflation expectations, real rates, and risk premia: Evidence from inflation swaps, *Review of Financial Studies* 25, 1588–1629.
- He, Zhiguo, Bryan Kelly, and Asaf Manela, 2017, Intermediary asset pricing: New evidence from many asset classes, *Journal of Financial Economics* 126, 1–35.
- He, Zhiguo, and Arvind Krishnamurthy, 2013, Intermediary asset pricing, *American Economic Review* 103, 732–70.
- He, Zhiguo, Stefan Nagel, and Zhaogang Song, 2022, Treasury inconvenience yields during the COVID-19 crisis, *Journal of Financial Economics* 143, 57–79.
- Hull, John, and Alan White, 2015, OIS discounting, interest rate derivatives, and the modeling of stochastic interest rate spreads, *Journal of Investment Management* 13, 64–83.
- Jermann, Urban, 2019, Is SOFR better than LIBOR?, Working Paper.
- Jermann, Urban, 2020a, Interest received by banks during the financial crisis: LIBOR vs hypothetical SOFR loans, Working Paper.
- Jermann, Urban, 2020b, Negative swap spreads and limited arbitrage, *Review of Financial Studies* 33, 212–238.
- Joslin, Scott, Anh Le, and Kenneth J. Singleton, 2013, Why Gaussian macro-finance term structure models are (nearly) unconstrained factor-VARs, *Journal of Financial Economics* 109, 604–622.
- Klingler, Sven, and Suresh Sundaresan, 2019, An explanation of negative swap spreads: Demand for duration from underfunded pension plans, *Journal of Finance* 74, 675–710.
- Klingler, Sven, and Olav Syrstad, 2021, Life after LIBOR, *Journal of Financial Economics* 141, 783–801.
- Krishnamurthy, Arvind, and Annette Vissing-Jorgensen, 2012, The aggregate demand for treasury debt, *Journal of Political Economy* 120, 233–267.
- Longstaff, Francis A., Pedro Santa-Clara, and Eduardo S. Schwartz, 2001, The relative valuation of caps and swaptions: Theory and empirical evidence, *Journal of Finance* 56, 2067–2109.
- Manela, Asaf, and Alan Moreira, 2017, News implied volatility and disaster concerns, *Journal of Financial Economics* 123, 137–162.
- McAndrews, James, Asani Sarkar, and Zhenyu Wang, 2017, The effect of the term auction facility on the London interbank offered rate, *Journal of Banking & Finance* 83, 135–152.
- Michaud, François-Louis, and Christian Upper, 2008, What drives interbank rates? Evidence from the Libor panel, *BIS Quarterly Review*.
- Munk, Claus, 1999, Stochastic duration and fast coupon bond option pricing in multi-factor models, *Review of Derivatives Research* 3, 157–181.

- Nelson, Charles R., and Andrew F. Siegel, 1987, Parsimonious modeling of yield curves, *Journal of Business* 60, 473–489.
- Newey, Whitney, and Kenneth West, 1987, A simple, positive semi-definite, heteroskedasticity and autocorrelation consistent covariance matrix, *Econometrica* 55, 703–708.
- Park, Yang-Ho, 2016, The effects of asymmetric volatility and jumps on the pricing of VIX derivatives, *Journal of Econometrics* 192, 313–328.
- Pastor, Lubos, and Robert F. Stambaugh, 2003, Liquidity risk and expected stock returns, *Journal of Political Economy* 111, 642–685.
- Reinhart, Carmen M., and Kenneth S. Rogoff, 2013, Banking crises: An equal opportunity menace, *Journal of Banking & Finance* 37, 4557–4573.
- Seo, Sang Byung, and Jessica A. Wachter, 2018, Do rare events explain CDX tranche spreads?, *Journal of Finance* 73, 2343–2383.
- Seo, Sang Byung, and Jessica A. Wachter, 2019, Option prices in a model with stochastic disaster risk, *Management Science* 65, 3449–3469.
- Taylor, John B., and John C. Williams, 2009, A black swan in the money market, *American Economic Journal: Macroeconomics* 1, 58–83.
- Trolle, Anders B., and Eduardo S. Schwartz, 2009, A general stochastic volatility model for the pricing of interest rate derivatives, *Review of Financial Studies* 22, 2007–2057.
- Tsai, Jerry, 2015, Rare disasters and the term structure of interest rates, Working paper.
- Wachter, Jessica A., 2013, Can time-varying risk of rare disasters explain aggregate stock market volatility?, *Journal of Finance* 68, 987–1035.
- Wan, Eric A., and Rudolph Van Der Merwe, 2000, The unscented Kalman filter for nonlinear estimation, *Proceedings of the IEEE 2000 Adaptive Systems for Signal Processing, Communications, and Control Symposium* pp. 153–158.
- Wei, Jason Z., 1997, A simple approach to bond option pricing, *Journal of Futures Markets: Futures, Options, and Other Derivative Products* 17, 131–160.

# Internet Appendix for

## “Options on Interbank Rates and Implied Disaster Risk”

### A Literature review

We provide detailed comparisons with related papers in three tables, highlighting our modeling innovations and empirical contributions. The first table juxtaposes our model and existing models of time-varying disaster risk. This comparison clearly shows how our work builds upon and differentiates itself from the existing literature. Notably, it emphasizes the reduced-form nature of our model, distinguishing it from equilibrium models. Additionally, the table shows that our parameter choices are estimated rather than calibrated. Our model also focuses on different asset classes, in contrast to prior models that are calibrated to match equity market moments.

	Model type	Parameter choices	Extracting disaster risk	Target asset classes
This paper	Reduced-form	Estimation	Yes	Interbank lending, caps, swaptions, nominal government bonds
Gabaix (2012)	Equilibrium	Calibration	No	Equity market, equity index options, nominal government/corporate bonds
Wachter (2013)	Equilibrium	Calibration	Yes	Equity market
Tsai (2015)	Equilibrium	Calibration	Yes	Equity market, nominal government bonds
Seo and Wachter (2018)	Equilibrium	Calibration	Yes	Equity market, equity index options, CDX tranches

The second table compares different ways in which time-varying disaster risk is characterized in the literature. Our relative advantage is that we can identify and extract the short-run



and long-run components of disaster risk, providing a more nuanced understanding of risk dynamics.

How time-varying disaster risk is characterized	
This paper	The short-run and long-run components of disaster risk are filtered through the unscented Kalman filter from interbank rates and options.
Berkman, Jacobsen, and Lee (2011)	A crisis severity index is constructed based on the number of international political crises.
Manela and Moreira (2017)	A disaster concern measure, called News implied volatility (NVIX), is calculated using textual analysis of newspaper articles.
Bakshi, Gao, and Xue (2023)	The disaster probability is computed from put option prices by solving a minimum discrepancy problem for the pricing kernel.

The third table compares our paper with prior studies on interest rate options. The table highlights that our model incorporates both stochastic volatility and jump components. It also juxtaposes the number of observable and unobservable state variables in each paper’s main model. The empirical methodologies are also summarized in the table, in terms of the filtering method, option pricing approach, and types of interest rate options used in the analyses.

	Stochastic volatility	Jump	Number of state variables		Filtering	Option pricing	Types of interest rate options
			Observable	Unobservable			
This paper	Yes	Yes	1	4	Unscented Kalman filter	Close-form solution	ATMF swaptions and caps
Longstaff, Santa-Clara, and Schwartz (2001)	No	No	0	4	Eigenvalue calculation	Simulation-based pricing	ATMF swaptions and caps
Han (2007)	Yes	No	0	3	Matching with observed prices	Close-form solution	ATMF swaptions and caps
Trolle and Schwartz (2009)	Yes	No	0	3	Extended Kalman filter	Close-form solution	ATMF swaptions and ATM, OTM and ITM caps
Bakshi, Crosby, Gao, and Hansen (2023)	Yes	No	0	5	Unscented Kalman filter	Simulation-based pricing	Treasury options

## B Unscented Kalman filter

As discussed in Section 3.2, we derive the discrete-time state equation based on the exact relation between  $S_t = [\lambda_t, \xi_t, \mu_t, x_t]^\top$  and  $S_{t-\Delta t} = [\lambda_{t-\Delta t}, \xi_{t-\Delta t}, \mu_{t-\Delta t}, x_{t-\Delta t}]^\top$ . To do so, we first integrate both sides of the stochastic differential equations for  $\lambda_t$ ,  $\xi_t$ ,  $\mu_t$ , and  $x_t$  from time  $t - \Delta t$  to time  $t$ :

$$\begin{aligned}\lambda_t &= \lambda_{t-\Delta t} + \kappa_\lambda \int_{t-\Delta t}^t (\xi_u - \lambda_u) du + \sigma_\lambda \int_{t-\Delta t}^t \sqrt{\lambda_u} dB_{\lambda,u}, \\ \xi_t &= \xi_{t-\Delta t} + \kappa_\xi \int_{t-\Delta t}^t (\bar{\xi} - \xi_u) du + \sigma_\xi \int_{t-\Delta t}^t \sqrt{\xi_u} dB_{\xi,u}, \\ \mu_t &= \mu_{t-\Delta t} + \kappa_\mu \int_{t-\Delta t}^t (\bar{\mu} - \mu_u) du + \sigma_\mu \int_{t-\Delta t}^t dB_{\mu,u}, \\ x_t &= x_{t-\Delta t} + \kappa_x \int_{t-\Delta t}^t (\bar{x} - \mu_u) du + \sigma_x \int_{t-\Delta t}^t dB_{x,u}.\end{aligned}$$

Note that an Ito integral is a martingale and, hence, its conditional mean is zero. By taking the conditional expectations  $\mathbb{E}_{t-\Delta t}[\cdot]$  on both sides of the equations, we simply obtain  $\mathbb{E}_{t-\Delta t}[S_t] = \eta + \Psi S_{t-\Delta t}$ , where

$$\begin{aligned}\eta &= \begin{bmatrix} -\frac{\kappa_\lambda \bar{\xi}}{\kappa_\lambda - \kappa_\xi} (e^{-\kappa_\xi \Delta t} - e^{-\kappa_\lambda \Delta t}) + \bar{\xi} (1 - e^{-\kappa_\lambda \Delta t}) \\ \bar{\xi} (1 - e^{-\kappa_\xi \Delta t}) \\ \bar{\mu} (1 - e^{-\kappa_\mu \Delta t}) \\ \bar{x} (1 - e^{-\kappa_x \Delta t}) \end{bmatrix}, \\ \Psi &= \begin{bmatrix} e^{-\kappa_\lambda \Delta t} & \frac{\kappa_\lambda}{\kappa_\lambda - \kappa_\xi} (e^{-\kappa_\xi \Delta t} - e^{-\kappa_\lambda \Delta t}) & 0 & 0 \\ 0 & e^{-\kappa_\xi \Delta t} & 0 & 0 \\ 0 & 0 & e^{-\kappa_\mu \Delta t} & 0 \\ 0 & 0 & 0 & e^{-\kappa_x \Delta t} \end{bmatrix}.\end{aligned}$$

This relation allows us to express  $S_t$  as in equation (13):

$$S_t = \mathbb{E}_{t-\Delta t}[S_t] + \epsilon_t, \quad \text{where } \mathbb{E}_{t-\Delta t}[\epsilon_t] = 0 \text{ and } \text{Var}_{t-\Delta t}[\epsilon_t] = \Omega_{t-\Delta t},$$

where the  $4 \times 4$  covariance matrix  $\Omega_{t-\Delta t}$  is given by

$$\Omega_{t-\Delta t} = \begin{bmatrix} \Omega_{\lambda\lambda,t-\Delta t} & \Omega_{\lambda\xi,t-\Delta t} & 0 & 0 \\ \Omega_{\lambda\xi,t-\Delta t} & \Omega_{\xi\xi,t-\Delta t} & 0 & 0 \\ 0 & 0 & \Omega_{\mu\mu,t-\Delta t} & 0 \\ 0 & 0 & 0 & \Omega_{xx,t-\Delta t} \end{bmatrix}.$$

Clearly,  $\epsilon_t$  is non-normal. However, in order to use a conventional filtering approach, we approximate it by a mean-zero normal random variable with the same covariance matrix  $\Omega_{t-\Delta t}$ .<sup>1</sup> We find each element of  $\Omega_{t-\Delta t}$  by considering the marginal and joint dynamics of  $\lambda_t$ ,  $\xi_t$ ,  $\mu$ , and  $x_t$ :

$$\begin{aligned} \Omega_{\lambda\lambda,t-\Delta t} &= \frac{\kappa_\lambda^2 \sigma_\xi^2 \xi_{t-\Delta t}}{(\kappa_\lambda - \kappa_\xi)^2 \kappa_\xi} (e^{-\kappa_\xi \Delta t} - e^{-2\kappa_\xi \Delta t}) + \frac{\kappa_\lambda^2 \bar{\xi} \sigma_\xi^2}{2(\kappa_\lambda - \kappa_\xi)^2 \kappa_\xi} (1 - e^{-\kappa_\xi \Delta t})^2 \\ &\quad - \frac{2\kappa_\lambda \sigma_\xi^2 (\xi_{t-\Delta t} - \bar{\xi})}{(\kappa_\lambda - \kappa_\xi)^2} (e^{-\kappa_\xi \Delta t} - e^{-(\kappa_\lambda + \kappa_\xi) \Delta t}) - \frac{2\kappa_\lambda^2 \sigma_\xi^2 \bar{\xi}}{(\kappa_\lambda - \kappa_\xi)^2 (\kappa_\xi + \kappa_\lambda)} (1 - e^{-(\kappa_\lambda + \kappa_\xi) \Delta t}) \\ &\quad + \frac{\kappa_\lambda^2 \sigma_\xi^2 (\xi_{t-\Delta t} - \bar{\xi})}{(\kappa_\lambda - \kappa_\xi)^2 (2\kappa_\lambda - \kappa_\xi)} (e^{-\kappa_\xi \Delta t} - e^{-2\kappa_\lambda \Delta t}) + \frac{\kappa_\lambda \sigma_\xi^2 \bar{\xi}}{2(\kappa_\lambda - \kappa_\xi)^2} (1 - e^{-2\kappa_\lambda \Delta t}) \\ &\quad + \frac{(\lambda_{t-\Delta t} - \bar{\xi}) \sigma_\lambda^2}{\kappa_\lambda} (e^{-\kappa_\lambda \Delta t} - e^{-2\kappa_\lambda \Delta t}) + \frac{\kappa_\lambda (\xi_{t-\Delta t} - \bar{\xi}) \sigma_\lambda^2}{(\kappa_\lambda - \kappa_\xi) (2\kappa_\lambda - \kappa_\xi)} (e^{-\kappa_\xi \Delta t} - e^{-2\kappa_\lambda \Delta t}) \\ &\quad - \frac{(\xi_{t-\Delta t} - \bar{\xi}) \sigma_\lambda^2}{\kappa_\lambda - \kappa_\xi} (e^{-\kappa_\lambda \Delta t} - e^{-2\kappa_\lambda \Delta t}) + \frac{\bar{\xi} \sigma_\lambda^2}{2\kappa_\lambda} (1 - e^{-2\kappa_\lambda \Delta t}), \\ \Omega_{\xi\xi,t-\Delta t} &= \frac{\sigma_\xi^2 \xi_{t-\Delta t}}{\kappa_\xi} (e^{-\kappa_\xi \Delta t} - e^{-2\kappa_\xi \Delta t}) + \frac{\sigma_\xi^2 \bar{\xi}}{2\kappa_\xi} (1 - e^{-\kappa_\xi \Delta t})^2, \\ \Omega_{\lambda\xi,t-\Delta t} &= \frac{\kappa_\lambda}{\kappa_\lambda - \kappa_\xi} \Omega_{\xi\xi,t-\Delta t} \\ &\quad - \frac{\sigma_\xi^2 (\xi_{t-\Delta t} - \bar{\xi})}{\kappa_\lambda - \kappa_\xi} (e^{-\kappa_\xi \Delta t} - e^{-(\kappa_\lambda + \kappa_\xi) \Delta t}) - \frac{\kappa_\lambda \sigma_\xi^2 \bar{\xi}}{(\kappa_\lambda - \kappa_\xi) (\kappa_\lambda + \kappa_\xi)} (1 - e^{-(\kappa_\lambda + \kappa_\xi) \Delta t}), \\ \Omega_{\mu\mu,t-\Delta t} &= \frac{\sigma_\mu^2}{2\kappa_\mu} (1 - e^{-2\kappa_\mu \Delta t}), \\ \Omega_{xx,t-\Delta t} &= \frac{\sigma_x^2}{2\kappa_x} (1 - e^{-2\kappa_x \Delta t}). \end{aligned}$$

Since our measurement equation is not linear in the state variables, we adopt the unscented

---

<sup>1</sup>As discussed in Section 3.2, it is well known that the effect of this approximation is minimal.

Kalman filter. The predicted state vector and its variance at time  $t - \Delta t$  (i.e.,  $\hat{S}_{t|t-\Delta t}$  and  $P_{t|t-\Delta t}$ ) are given as follows:

$$\begin{aligned}\hat{S}_{t|t-\Delta t} &= \eta + \Psi \hat{S}_{t-\Delta t}, \\ P_{t|t-\Delta t} &= \Psi P_{t-\Delta t} \Psi' + \Omega_{t-\Delta t}.\end{aligned}$$

We define sigma points that help capture the mean and variance of the latent state variables. Specifically, we select the following set of  $2L + 1$  sigma points ( $\mathcal{S}$ ) and weights ( $W^m$  for the mean and  $W^c$  for the covariance of the observations evaluated at the sigma points):

$$\begin{aligned}\mathcal{S}_0 &= \hat{S}_{t|t-\Delta t}, \\ \mathcal{S}_i &= \hat{S}_{t|t-\Delta t} + \left( \sqrt{(L + \chi) P_{t|t-\Delta t}} \right)_i, \quad i = 1, \dots, L, \\ \mathcal{S}_i &= \hat{S}_{t|t-\Delta t} - \left( \sqrt{(L + \chi) P_{t|t-\Delta t}} \right)_{i-L}, \quad i = L + 1, \dots, 2L,\end{aligned}$$

and

$$\begin{aligned}W_0^m &= \frac{\chi}{L + \chi}, \\ W_0^c &= \frac{\chi}{L + \chi} + (1 - \alpha^2 + \beta), \\ W_i^m = W_i^c &= \frac{1}{2(L + \chi)}, \quad i = 1, \dots, 2L,\end{aligned}$$

where  $L$  is the number of the latent variables,  $\chi = \alpha^2(L + \kappa) - L$  is a scaling parameter, and  $\left( \sqrt{(L + \chi) P_{t|t-\Delta t}} \right)_i$  is the  $i$ -th column of the matrix square root. In this paper, we use  $\alpha = 0.01$ ,  $\beta = 2$ , and  $\kappa = 0$ .

The mean and covariance of the predicted vector  $\hat{Y}_t$  are computed using a weighted mean

and covariance of the sigma points:

$$\begin{aligned}\hat{Y}_{t|t-\Delta t} &= \sum_{i=0}^{2L} W_i^m h(\mathcal{S}_i), \\ P_{t|t-\Delta t}^y &= \sum_{i=0}^{2L} W_i^c \left( h(\mathcal{S}_i) - \hat{Y}_{t|t-\Delta t} \right) \left( h(\mathcal{S}_i) - \hat{Y}_{t|t-\Delta t} \right)' + Q.\end{aligned}$$

Then, we obtain the filtered state vector at time  $t$  (i.e.,  $\hat{S}_t$ ) as follows:

$$\begin{aligned}\hat{S}_t &= \hat{S}_{t|t-\Delta t} + K_t \hat{e}_t, \\ P_t &= P_{t|t-\Delta t} - K_t P_{t|t-\Delta t}^y K_t',\end{aligned}$$

where

$$\begin{aligned}K_t &= \sum_{i=0}^{2L} W_i^c \left( \mathcal{S}_i - \hat{S}_{t|t-\Delta t} \right) \left( h(\mathcal{S}_i) - \hat{Y}_{t|t-\Delta t} \right)' \left( P_{t|t-\Delta t}^y \right)^{-1}, \\ \hat{e}_t &= Y_t - \hat{Y}_{t|t-\Delta t}.\end{aligned}$$

For the initial month, the values of  $\hat{S}_{t-\Delta t}$  and  $P_{t-\Delta t}$  are set to be the unconditional mean and variance of  $S_t$ . The Kalman filter recursion also enables us to calculate the likelihood of observing  $Y_t$  conditional on  $Y_{t-\Delta t}$ :

$$\log \mathcal{L}_t = -\frac{l}{2} \log(2\pi) - \frac{1}{2} \log |P_{t|t-\Delta t}^y| - \frac{1}{2} \hat{e}_t' \left( P_{t|t-\Delta t}^y \right)^{-1} \hat{e}_t,$$

where  $l$  is the size of the vector  $Y_t$ .

## C Estimation of nested models

The key feature of our model is disaster risk, which consists of time-varying short-run and long-run components. To demonstrate the importance of disaster risk, we examine two nested cases: (i) constant long-run mean of disaster risk (i.e., no variation in  $\xi_t$ ) where  $\kappa_\xi = \sigma_\xi = \delta_\xi = \theta_\xi = 0$ ; (ii) constant disaster risk (i.e., no variation in  $\lambda_t$ ) where  $\kappa_\xi = \kappa_\lambda = \sigma_\xi = \sigma_\lambda = \delta_\xi = \delta_\lambda = \theta_\xi = \theta_\lambda = 0$ . It is important to note that we do not consider a specification without disaster risk (no jump component at all) because, in the absence of disaster risk, the interbank rate would collapse to the OIS rate under our model setup. Parameter estimates for both alternative models are presented in the tables below:

**Nested case (i):** Constant long-run mean of disaster risk

		$\kappa_\mu$	$\sigma_\mu$	$\sigma_C$	$\bar{\mu}$
Consumption growth	Est. (SE)	0.0687 (0.0003)	0.0035 (0.0000)	0.0078 (0.0001)	0.0105
Expected inflation	Est. (SE)	$\kappa_q$ 0.5239 (0.3153)	$\sigma_q$ 0.0065 (0.0011)	$\bar{q}$ 0.0212 (0.0028)	
Disaster risk	Est. (SE)	$\kappa_\lambda$ 0.4252 (0.0030)	$\sigma_\lambda$ 0.1385 (0.0003)	$\bar{p}$ 0.9214 (0.0076)	$\bar{\xi}$ 0.0286
Convenience yield	Est. (SE)	$\kappa_x$ 0.8162 (0.1915)	$\sigma_x$ 0.0017 (0.0003)	$\bar{x}$ 0.0021 (0.0004)	
Short rate	Est. (SE)	$\delta_\lambda$ -0.1004 (0.0005)	$\delta_q$ 0.4253 (0.0024)	$\delta_\mu$ 2.4470 (0.0224)	$\delta_0$ -0.0174
Market price of risk	Est. (SE)	$\theta_\lambda$ -0.1381 (0.0005)	$\theta_q$ -4.2443 (0.0288)	$\theta_\mu$ 0.1968 (0.0008)	$\theta_N$ -0.1699 (0.0009)
Measurement errors	Est. (SE)	$\sigma_{SP}$ 0.0016 (0.0000)	$\sigma_{ITR}$ 0.0033 (0.0000)	$\sigma_{OPT}$ 0.0745 (0.0007)	

One notable observation from the estimation of these two nested models is that the parameter estimates of  $\kappa_\mu$  are much smaller than that in our main specification in Table 2. These estimates are around 0.05, which is similar to the estimate of  $\kappa_\xi$  in Table 2. This finding suggests that a very highly persistent state variable is required to capture the time

**Nested case (ii):** Constant disaster risk

		$\kappa_\mu$	$\sigma_\mu$	$\sigma_C$	$\bar{\mu}$
Consumption growth	Est. (SE)	0.0435 (0.0007)	0.0042 (0.0001)	0.0077 (0.0001)	0.0105
Expected inflation	Est. (SE)	$\kappa_q$ 0.5239 (0.3153)	$\sigma_q$ 0.0065 (0.0011)	$\bar{q}$ 0.0212 (0.0028)	
Disaster risk	Est. (SE)	$\bar{p}$ 0.8496 (0.0063)	$\xi$ 0.0286		
Convenience yield	Est. (SE)	$\kappa_x$ 0.8162 (0.1915)	$\sigma_x$ 0.0017 (0.0003)	$\bar{x}$ 0.0021 (0.0004)	
Short rate	Est. (SE)	$\delta_q$ 0.5744 (0.0077)	$\delta_\mu$ 2.1526 (0.0461)	$\delta_0$ -0.0203	
Market price of risk	Est. (SE)	$\theta_q$ -2.8155 (0.0415)	$\theta_\mu$ 0.1174 (0.0011)	$\theta_N$ -0.0880 (0.0005)	
Measurement errors	Est. (SE)	$\sigma_{SP}$ 0.0038 (0.0000)	$\sigma_{ITR}$ 0.0039 (0.0003)	$\sigma_{OPT}$ 0.0736 (0.0010)	

series of interest rates and option-implied volatilities. Since  $\xi_t$  is no longer time-varying in the nested models, the persistence of  $\mu_t$  is artificially forced to be very high. The omission of time-varying  $\xi_t$  increases the measurement error in interest rates by 13 to 19 basis points. When  $\lambda_t$  is held constant, the measurement error in interest rate spreads more than doubles.

In addition to the two cases related to disaster risk, we consider a third nested model: (iii) absence of expected inflation, where we set  $\kappa_q = \sigma_q = \bar{q} = \delta_q = \theta_q = 0$ . While expected inflation plays a crucial role in capturing the level of interest rates in the full model, its omission is not impossible given the reduced-form nature of our framework. The corresponding parameter estimates are reported in the table below.

Given that these alternative models are nested within our main model specification, we conduct a likelihood ratio test to compare their performance. The table below reports the log-likelihood for the full model alongside those for the three nested models. Under the null of no difference between the main model and each nested model, the likelihood ratio test statistic  $2 \times (\log \mathcal{L} - \log \mathcal{L}_{\text{nested}})$  should follow a chi-square distribution with degrees of freedom equal

**Nested case (iii):** Absence of expected inflation

		$\kappa_\mu$	$\sigma_\mu$	$\sigma_C$	$\bar{\mu}$
Consumption growth	Est. (SE)	0.5799 (0.0098)	0.0056 (0.0002)	0.0086 (0.0001)	0.0105
<hr/>					
		$\kappa_\xi$	$\sigma_\xi$	$\bar{\xi}$	
Disaster risk	Est. (SE)	0.0442 (0.0009)	0.0215 (0.0001)	0.0286	
		$\kappa_\lambda$	$\sigma_\lambda$	$\bar{p}$	
	Est. (SE)	0.4472 (0.0067)	0.1749 (0.0006)	0.8824 (0.0220)	
<hr/>					
		$\kappa_x$	$\sigma_x$	$\bar{x}$	
Convenience yield	Est. (SE)	0.8162 (0.1915)	0.0017 (0.0003)	0.0021 (0.0004)	
<hr/>					
		$\delta_\lambda$	$\delta_\xi$	$\delta_\mu$	$\delta_0$
Short rate	Est. (SE)	-0.1294 (0.0020)	-2.1165 (0.0119)	1.9295 (0.0087)	0.0581
<hr/>					
		$\theta_\lambda$	$\theta_\xi$	$\theta_\mu$	$\theta_N$
Market price of risk	Est. (SE)	-0.1190 (0.0008)	-0.2655 (0.0008)	0.1015 (0.0027)	-0.1386 (0.0035)
<hr/>					
		$\sigma_{SP}$	$\sigma_{ITR}$	$\sigma_{OPT}$	
Measurement errors	Est. (SE)	0.0014 (0.0000)	0.0022 (0.0000)	0.0776 (0.0007)	

to the number of restrictions. The table shows that the resulting  $p$ -values are virtually zero, rejecting the nested models and thereby supporting our original specification.

	Main	(i) Constant $\xi$	(ii) Constant $\lambda$	(iii) Without $q$
$\log \mathcal{L}$	26,741.17	25,160.56	23,897.70	26,386.13
$p$ -value		0.00	0.00	0.00



## D Equivalent bond price volatility

In Figure 3, the Black-implied volatilities for the 2-year cap are generally much higher than those for the 5-year cap. Furthermore, in all of the panels in Figure 3, the Black-implied volatilities between 2010 and 2016 are exceptionally high even compared to the Great Recession period between 2007 and 2009.

Why do the time series and cross sectional patterns of Black-implied volatilities seem odd? The reason is that Black-implied volatilities for caps and swaptions, converted from their market prices through the Black formulas, represent yield volatilities, not bond price volatilities. Hence, the level of Black-implied volatilities simply tends to be higher when the level of interest rates is lower. This explains why Black-implied volatilities in the data turn out to be so high in the post Great Recession period despite relatively lower uncertainty in the market: a 1% expected movement in a yield corresponds to 20% yield volatility if the yield is currently at 5%, whereas it corresponds to 100% if the yield is at 1%.

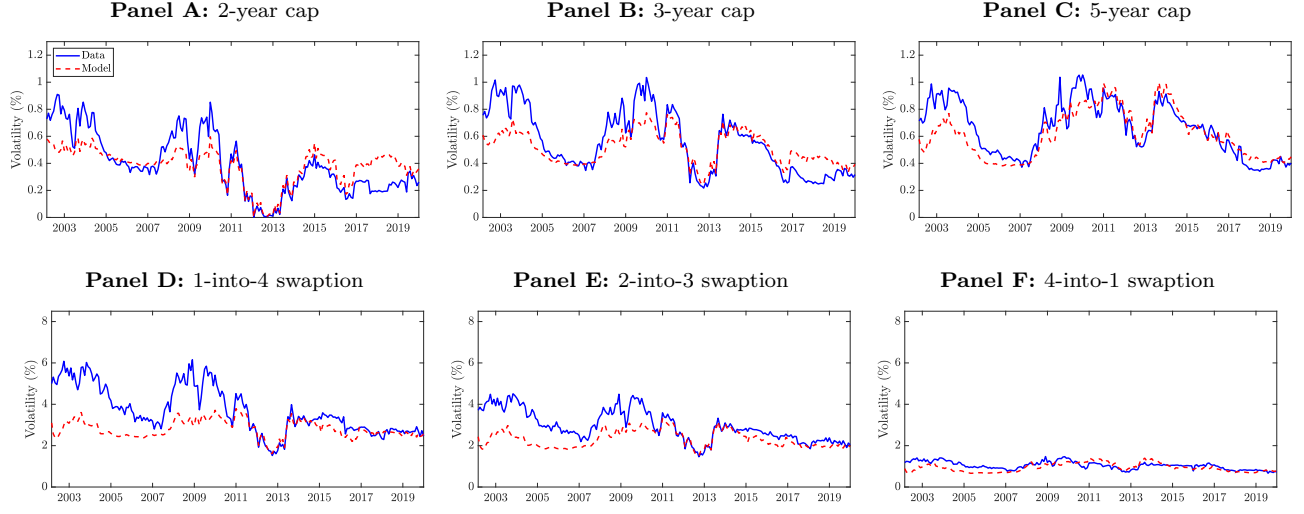
To facilitate interpretation, it is possible to convert each Black-implied volatility into its equivalent price volatility. Under the Black model, forward yield volatility  $\sigma_{\text{yield}}$  shares the following relation with forward-starting bond price volatility  $\sigma_{\text{price}}$ :

$$\sigma_{\text{price}} = \tau \times y \times \sigma_{\text{yield}},$$

where, with a slight abuse of notation,  $\tau$  is the maturity of the bond and  $y$  is the given (forward) yield. Using this simple relation, we can convert the Black-implied volatilities in the data and in the model into their equivalent forward-starting bond price volatilities.

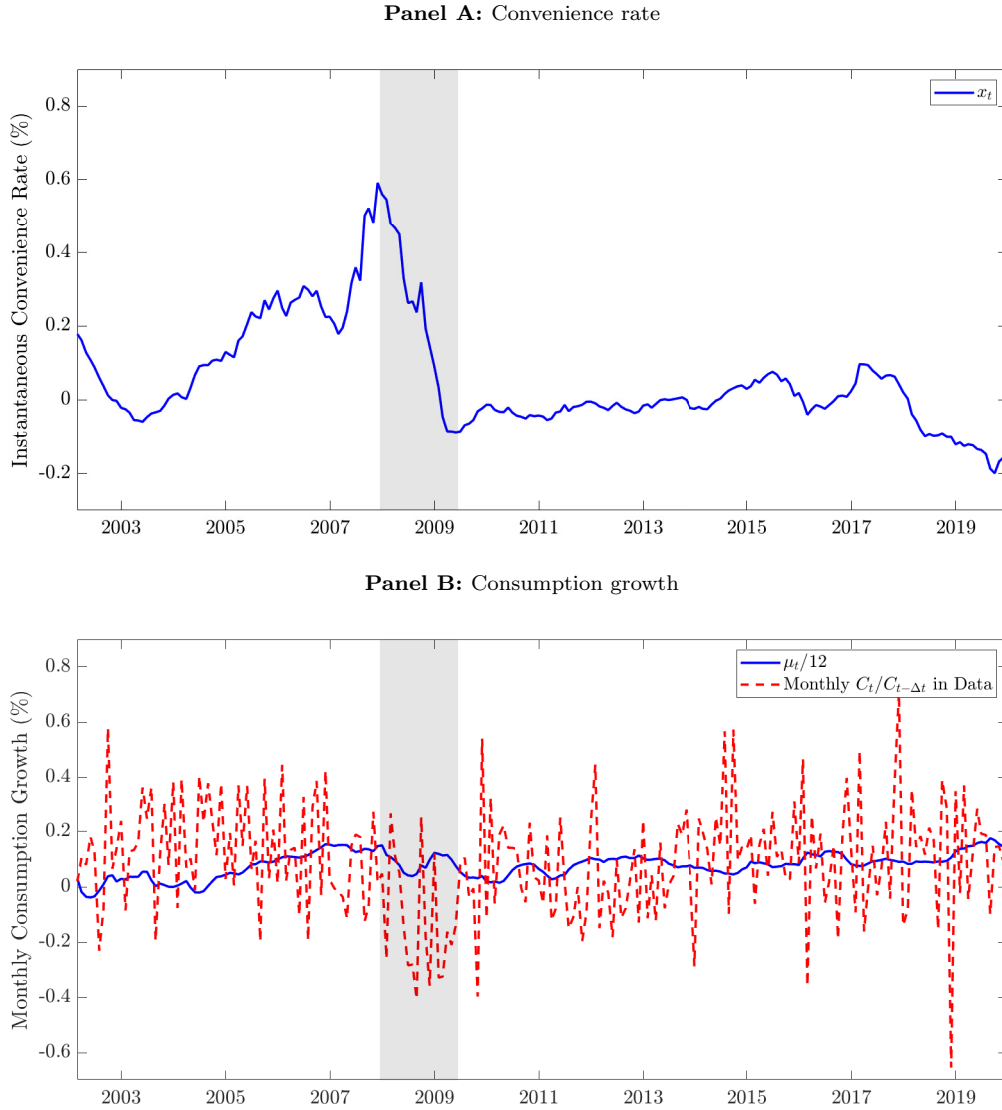
The figure below plots the time series of the equivalent bond price volatilities for the 2-, 3-, and 5-year caps (Panels A, B, and C) and those for the 1-into-4, 2-into-3, and 4-into-1 swaptions (Panels D, E, and F) in the data (solid blue lines) and in the model (dashed red lines). The Black-implied volatility for the  $T$ -maturity cap is converted into the price volatility of a bond that corresponds to its last caplet: a 6-month zero-coupon bond starting after  $(T - 0.5)$  years and maturing after  $T$  years from today. The Black-implied volatility for

the  $T$ -into- $\bar{T}$  swaption is converted to the price volatility of a  $\bar{T}$ -maturity zero-coupon bond starting  $T$  years from today. The sample period is from February 2002 to December 2019.



## E Filtered time series of $x_t$ and $\mu_t$

The figure below presents the filtered time series of the instantaneous convenience rate  $x_t$  (Panel A) and mean consumption growth per month  $\mu_t/12$  (Panel B) from February 2002 to December 2019. In Panel B, we overlay the time series of monthly mean consumption growth (solid blue line) with that of monthly realized consumption growth (dashed red line). Summary statistics for each time series are also reported.

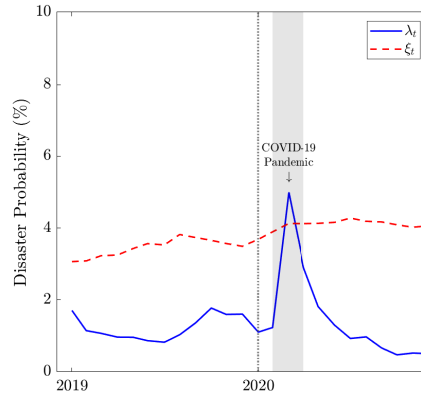


	Mean	SD	Min	5th	50th	95th	Max
$x$	0.06	0.15	-0.20	-0.12	0.00	0.33	0.59
$\mu$	0.94	0.53	-0.46	0.01	1.00	1.81	2.11

## F COVID-19 pandemic crisis

In 2020, the global economy and financial markets were severely impacted by the COVID-19 pandemic crisis. What do interbank rates and their options imply about this crisis through our model framework?

We extend our data sample and examine how the implied short-run and long-run components of disaster risk progressed over the pandemic period. Based on the estimated parameters in Table 2, we apply the unscented Kalman filter from Section 3.2 to the additional data from January 2020 to December 2020. The figure below plots the resulting time series of filtered  $\lambda_t$  (solid blue line) and  $\xi_t$  (dashed red line).



The figure reveals that the long-run component  $\xi_t$  slightly increased at the onset of the crisis and remained elevated throughout 2020 (4.1% in December). In contrast, the short-run component  $\lambda_t$  exhibited drastic changes over the period. Until February,  $\lambda_t$  stayed at a low level of around 1%, but it jumped up to 5.0% in March. This was followed by an abrupt decline in April and May, pushing  $\lambda_t$  quickly back to its pre-pandemic level. Overall, the figure suggests that, at least through our model framework, the COVID-19 pandemic resulted in a very short-lived economic/financial crisis, despite its long-lasting impacts. This interpretation is in line with the view of the Business Cycle Dating Committee of the NBER; the committee determined that the pandemic-originated recession only lasted for two months (March and April), making it the shortest U.S. recession ever documented.

## G Structure of bond price volatility

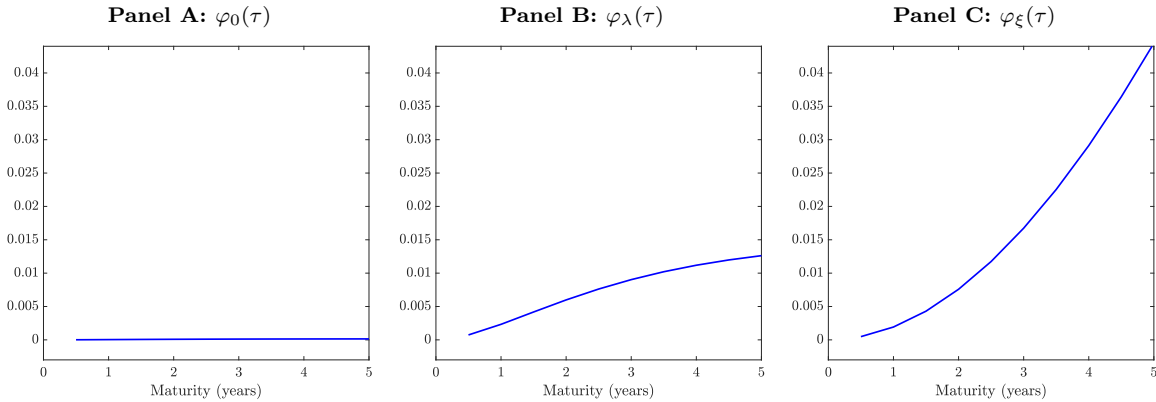
In our model, the bond volatility is a function of the two disaster state variables  $\lambda_t$  and  $\xi_t$ . More formally, let  $P_i(t, t + \tau)$  denote the price of a zero-coupon interbank lending where  $\tau$  is the bond maturity. By Ito's lemma, the price dynamics under the physical measure can be expressed as follows:

$$\begin{aligned} \frac{dP_{i,t}}{P_{i,t-}} = & \mu_{P_{i,t}} dt + b_{i,\lambda}(\tau) \sigma_\lambda \sqrt{\lambda_t} dB_{\lambda,t} + b_{i,\xi}(\tau) \sigma_\xi \sqrt{\xi_t} dB_{\xi,t} \\ & + b_{i,\mu}(\tau) \sigma_\mu dB_{\mu,t} + b_{i,q}(\tau) \sigma_q dB_{q,t} + (e^{b_{i,q}(\tau) Z_{q,t}} - 1) dN_t. \end{aligned}$$

This implies that the instantaneous bond volatility is calculated by

$$\frac{d\text{Var}_t(\log P_{it})}{dt} = \underbrace{(b_{i,q}^2(\tau) \sigma_q^2 + b_{i,\mu}^2(\tau) \sigma_\mu^2)}_{\varphi_0(\tau)} + \underbrace{(b_\lambda^2(\tau) \sigma_\lambda^2 + b_{i,q}^2(\tau) E_t[Z_{q,t}^2])}_{\varphi_\lambda(\tau)} \lambda_t + \underbrace{b_\xi^2(\tau) \sigma_\xi^2}_{\varphi_\xi(\tau)} \xi_t.$$

The figure below plots the two factor loadings  $\varphi_\lambda(\tau)$  and  $\varphi_\xi(\tau)$ , as well as the intercept term  $\varphi_0(\tau)$ , as functions of  $\tau$ . While we can see that the intercept term is very small and does not vary much with maturity (Panel A), the two factor loadings increase monotonically (Panels B and C). Comparing the two, the factor loading for  $\xi_t$  rises much faster with a steeper slope than that for  $\lambda_t$ . The rate of increase is also larger;  $\varphi_\xi(\tau)$  is convex in  $\tau$ , whereas  $\varphi_\lambda(\tau)$  is concave. This is intuitive since the long-run component of disaster risk has a greater effect on long-term rates, which leads to a larger impact on the variance of long-term bonds.



# References for the Internet Appendix

- Bakshi, Gurdip, John Crosby, Xiaohui Gao, and Jorge W. Hansen, 2023, Treasury option returns and models with unspanned risks, *Journal of Financial Economics* 150, 103736.
- Bakshi, Gurdip, Xiaohui Gao, and Jinming Xue, 2023, Recovery with applications to forecasting equity disaster probability and testing the spanning hypothesis in the treasury market, *Journal of Financial and Quantitative Analysis* pp. 1–35.
- Berkman, Henk, Ben Jacobsen, and John B. Lee, 2011, Time-varying rare disaster risk and stock returns, *Journal of Financial Economics* 101, 313–332.
- Gabaix, Xavier, 2012, An exactly solved framework for ten puzzles in macro-finance, *Quarterly Journal of Economics* 127, 645–700.
- Han, Bing, 2007, Stochastic volatilities and correlations of bond yields, *Journal of Finance* 62, 1491–1524.
- Longstaff, Francis A., Pedro Santa-Clara, and Eduardo S. Schwartz, 2001, The relative valuation of caps and swaptions: Theory and empirical evidence, *Journal of Finance* 56, 2067–2109.
- Manela, Asaf, and Alan Moreira, 2017, News implied volatility and disaster concerns, *Journal of Financial Economics* 123, 137–162.
- Seo, Sang Byung, and Jessica A. Wachter, 2018, Do rare events explain CDX tranche spreads?, *Journal of Finance* 73, 2343–2383.
- Trolle, Anders B., and Eduardo S. Schwartz, 2009, Unspanned stochastic volatility and the pricing of commodity derivatives, *Review of Financial Studies* 22, 4423–4461.
- Tsai, Jerry, 2015, Rare disasters and the term structure of interest rates, Working paper.
- Wachter, Jessica A., 2013, Can time-varying risk of rare disasters explain aggregate stock market volatility?, *Journal of Finance* 68, 987–1035.